PCT

WORLD INTELLECTUAL PROPERTY ORGANIZATION
International Bureau

B6

INTERNATIONAL APPLICATION PUBLISHED UNDER THE PATENT COOPERATION TREATY (PCT)

(51) International Patent Classification 6 : C07H 21/00

A1

(11) International Publication Number: WO 98/27104

(43) International Publication Date: 25 June 1998 (25.06.98)

(21) International Application Number: PCT/US97/24158

(22) International Filing Date: 18 December 1997 (18.12.97)

(30) Priority Data:

60/033,684	19 December 1996 (19.12.96)	US
60/055,039	8 August 1997 (08.08.97)	US

(81) Designated States: AU, CA, JP, US, European patent (AT, BE, CH, DE, DK, ES, FI, FR, GB, GR, IE, IT, LU, MC, NL, PT, SE).

Published

With international search report.

Before the expiration of the time limit for amending the claims and to be republished in the event of the receipt of amendments.

(71) Applicant *(for all designated States except US)*: YALE UNIVERSITY [US/US]; Office of Cooperative Research, 155 Whitney Avenue, New Haven, CT 06520–8336 (US).

(72) Inventor; and

(75) Inventor/Applicant *(for US only)*: BREAKER, Ronald, R. [US/US]; 71 Hiddlen Lane, Guildord, CT 06437 (US).

(74) Agent: KRINSKY, Mary, M.; 88 Prospect Street, New Haven, CT 06511–3797 (US).

(54) Title: BIOREACTIVE ALLOSTERIC POLYNUCLEOTIDES

(57) Abstract

Polynucleotides having allosteric properties that modify a function or configuration of the polynucleotide with a chemical effector and/or physical signal are employed primarily as biosensors and/or enzymes for diagnostic and catalytic purposes. In some preferred embodiments, the polynucleotides are DNA enzymes that are used in solution/suspension or attached to a solid support as biosensors to detect the presence or absence of a compound, its concentration, or physical change in a sample by observation of self–catalysis. Chemical effectors include organic compounds such as amino acids, amino acid derivatives, peptides, nucleosides, nucleotides, steroids, and mixtures of these with each other and with metal ions, cellular metabolites or blood components obtained from biological samples, steroids, pharmaceuticals, pesticides, herbicides, food toxins, and the like. Physical signals include radiation, temperature changes, and combinations thereof.

FOR THE PURPOSES OF INFORMATION ONLY

Codes used to identify States party to the PCT on the front pages of pamphlets publishing international applications under the PCT.

AL	Albania
AM	Armenia
AT	Austria
AU	Australia
AZ	Azerbaijan
BA	Bosnia and Herzegovina
BB	Barbados
BE	Belgium
BF	Burkina Faso
BG	Bulgaria
BJ	Benin
BR	Brazil
BY	Belarus
CA	Canada
CF	Central African Republic
CG	Congo
CH	Switzerland
CI	Côte d'Ivoire
CM	Cameroon
CN	China
CU	Cuba
CZ	Czech Republic
DE	Germany
DK	Denmark
EE	Estonia
ES	Spain
FI	Finland
FR	France
GA	Gabon
GB	United Kingdom
GE	Georgia
GH	Ghana
GN	Guinea
GR	Greece
HU	Hungary
IE	Ireland
IL	Israel
IS	Iceland
IT	Italy
JP	Japan
KE	Kenya
KG	Kyrgyzstan
KP	Democratic People's Republic of Korea
KR	Republic of Korea
KZ	Kazakstan
LC	Saint Lucia
LI	Liechtenstein
LK	Sri Lanka
LR	Liberia
LS	Lesotho
LT	Lithuania
LU	Luxembourg
LV	Latvia
MC	Monaco
MD	Republic of Moldova
MG	Madagascar
MK	The former Yugoslav Republic of Macedonia
ML	Mali
MN	Mongolia
MR	Mauritania
MW	Malawi
MX	Mexico
NE	Niger
NL	Netherlands
NO	Norway
NZ	New Zealand
PL	Poland
PT	Portugal
RO	Romania
RU	Russian Federation
SD	Sudan
SE	Sweden
SG	Singapore
SI	Slovenia
SK	Slovakia
SN	Senegal
SZ	Swaziland
TD	Chad
TG	Togo
TJ	Tajikistan
TM	Turkmenistan
TR	Turkey
TT	Trinidad and Tobago
UA	Ukraine
UG	Uganda
US	United States of America
UZ	Uzbekistan
VN	Viet Nam
YU	Yugoslavia
ZW	Zimbabwe

BIOREACTIVE ALLOSTERIC POLYNUCLEOTIDES

Related Application Data

This application claims priority benefit of U.S. provisional patent application serial number 60/033,684, filed December 19, 1996, and U.S. provisional patent application serial number 60/055,039, filed August 8, 1997.

Technical Field of the Invention

This invention relates primarily to functional DNA polynucleotides that exhibit allosteric properties, and to catalytic RNA and DNA polynucleotides that have catalytic properties with rates that can be controlled by a chemical effector, a physical signal, or combinations thereof. Bioreactive allosteric polynucleotides of the invention are useful in a variety of applications, particularly as biosensors.

Biosensors are widely used in medicine, veterinary medicine, industry, and environmental science, especially for diagnostic purposes. Biosensors are typically composed of a biological compound (sensor material) that is coupled to a transducer, in order to produce a quantitative readout of the agent or conditions under analysis. Usually, the biological component of the biosensor is a macromolecule, often subject to a conformational change upon recognition and binding of its corresponding ligand. In nature, this effect may immediately initiate a signal process (*e.g.*, ion channel function in nerve cells). Included in the group of 'affinity sensors' are lectins, antibodies, receptors, and oligonucleotides. In biosensors, ligand binding to the affinity sensor is detected by optoelectronic devices, potentiometric electrodes, field effect transistors (FETs), or the like.

Alternatively, the specificity and catalytic power of proteins have been harnessed to create biosensors that operate via enzyme function. Likewise, proteins have been used as immobilized catalysts for various industrial applications. The catalytic activity of purified enzymes or even whole organelles, microorganisms or tissues can be monitored by potentiometric or amperometric electrodes, FETs, or thermistors. The majority of biosensors that are commercially available are based on enzymes, of which the oxidoreductases and lyases are of great interest. It is nearly exclusively the reactants of the reactions catalyzed by these enzymes for which transducers are available. These transducers include potentiometric electrodes, FETs, pH- and O_2-sensitive probes, and amperometric electrodes for H_2O_2 and redox mediators. For example, the oxidoreductases, a group of enzymes that catalyze the transfer of redox equivalents, can be monitored by detectors that are sensitive to H_2O_2 or O_2 concentrations.

Enzymes are well-suited for application in sensing devices. The binding constants for many enzymes and receptors can be extremely low (*e.g.*, avidin; K_d = 10^{-15} M) and the catalytic rates are on the order of a few thousand per second, but can reach 600,000 sec^{-1} (carboanhydrase) (45). Enzymes can be monitored as biosensors via their ability to convert substrate to product, and also be the ability of certain analytes to act as inhibitors of catalytic function.

Organic chemistry and biochemistry have reached a state of proficiency where new molecules can be made to simulate the function of protein receptors and enzymes. Macrocyclic rings, polymers for imprinting, and self-assembling monolayers are now being intensively investigated for their potential application in biosensors. In addition, the immune system of animals can be harnessed to create new ligand-binding proteins that can act as artificial biorecognition systems. Antibodies that have been made to bind transition-state analogues can also catalyze chemical reactions, thereby functioning as novel 'artificial enzymes' (36). The latter examples are an important route to the creation of biosensors that can be used to detect non-natural compounds, or that function under non-physiologic conditions.

Background of the Invention

In nature, RNA not only serves as components of the information transfer process, but also performs tasks that are typically accomplished by proteins, including molecular recognition and catalysis. A seemingly endless variety of aptamers, and even DNA aptamers can be created *in vitro* that bind various ligands with great affinity and specificity (17). Nucleic acids likely have an extensive and as yet untapped ability adopt specific conformations that can bind ligands and also to catalyze chemical transformations (16). The engineering of new RNA and DNA receptors and catalysts is primarily achieved via *in vitro* selection, a method by which trillions of different oligonucleotide sequences are screened for molecules that display the desired function. This method consists of repeated rounds of selection and amplification in a manner that simulates Darwinian evolution, but with molecules and not with living organisms (4). One drawback to the use of existing enzymes as biosensors is that one is limited to developing a sensor based on the properties of existing enzymes or receptors. A significant advantage can be gained if one could 'tailor-make' the sensor for a particular application. It would be desirable to employ nucleic acids to create entirely new biosensors that have properties and specificities that span beyond the range of capabilities of current biosensors.

In vitro selection has been the main vehicle for new ribozyme discoveries in recent years. The catalytic repertoire of ribozymes includes RNA and DNA phosphoester hydrolysis and transesterification, RNA ligation, RNA phosphorylation, alkylation, amide and ester bond formation, and amide cleavage reactions. Recent evidence has shown that biocatalysis is not solely the realm of RNA and proteins. DNA has been shown to form catalytic structures that efficiently cleave RNA (5,7), that ligate DNA (10), and that catalyze the metallation of porphyrin rings (24). As described herein, self-cleaving DNAs have been isolated from a random-sequence pool of molecules that operate via a redox mechanism, making

possible the use of an artificial DNA enzyme in place of oxidoreductase enzymes in biosensors. In addition, these DNA enzymes or 'deoxyribozymes' are considerably more stable that either RNA or protein enzymes – an attractive feature for the sensor component of a biosensor device.

Summary of the Invention

It is an object of the invention to provide examples of RNA and DNA sensing elements for use in biosensors, including polynucleotides attached to a solid support. Both RNA and DNA can be designed to bind a variety of ligands with considerable specificity and affinity. In addition, both RNA and DNA can be made to catalyze chemical transformations under user-defined conditions. A combination of rational design and combinatorial methods has been used to create prototype biosensors based on RNA and DNA.

These and other objects of the invention are accomplished by the present invention, which provides purified functional DNA polynucleotides that exhibit allosteric properties that modify a function or configuration of the polynucleotide with a chemical effector, a physical signal, or combinations thereof. The invention further provides purified functional polynucleotides having catalytic properties with rates that can be controlled by a chemical effector, a physical signal, or combinations thereof. Some embodiments are enzymes exhibiting allosteric properties that modify the rate of catalysis of the enzyme. In addition, the invention encompasses biosensors comprising bioreactive allosteric polynucleotides described herein.

Examples of chemical effectors include, but are not limited to, organic compounds such as amino acids, amino acid derivatives, peptides, nucleosides, nucleosides, nucleotides, steroids, and mixtures of organic compounds and metal ions. In some embodiments, the effectors are microbial or cellular metabolites or components of bodily fluids such as blood and urine obtained from biological

samples. In other embodiments, the effectors are pharmaceuticals, pesticides, herbicides, and food toxins. Physical signals include, but are not limited to, radiation and temperature changes.

The invention also provides methods for determining the presence or absence of compounds, or compound concentrations in biological, industrial, and environmental samples, and physical changes in such samples using bioreactive allosteric polynucleotides of the invention and biosensors incorporating them.

Description of the Figures

Figure 1 is a schematic diagram of an example of a biosensor of the invention. In this embodiment, a self-cleaving DNA is immobilized on a solid matrix that is mounted in a plastic 'spin-column'. The self-cleaving DNA remains inactive, unless it encounters a specific effector molecule that causes allosteric induction. Test sample is added to the porous matrix, allowed to incubate, then the solution is collected at the bottom of the tube via centrifugation. Since catalytic activity is a function of the presence (in concentration) of the effector, the concentration of released DNA fragments will report the presence and quantity of effector.

Figure 2 illustrates a sequence and secondary-structure model for a self-cleaving DNA of the invention (SEQ ID NO: 1). The bracket indicates the main region of DNA cleavage.

Figure 3 sketches an example of (A) an immobilized DNA biocatalyst of the invention and (B) a simple reactor assembly.

Figure 4 shows a demonstration of catalytic function by immobilized DNA enzymes. 5′ ^{32}P-labeled RNA substrate was applied to a streptavidin column (AffiniTip Strep 20, Genosys Biotechnologies) that was derivatized with 5′-biotinyl

DNA enzyme. The DNA enzyme was immobilized to give an effective concentration of ~ 1 μM. Substrate (0.5 μM was applied to the column in repetitive 20 μL aliquots, allowed to react for 10 min., then recovered for analysis by polyacrylamide gel electrophoresis. Fraction of substrate cleaved was plotted as a function of volume eluted.

Figure 5 illustrates hammerhead ribozyme constructs described in Example 1 below. **H1** (SEQ ID NO: 2) is identical to the ribozyme 'HH15' that was originally characterized by Fedor and Uhlenbeck (12). **H2** (SEQ ID NO: 3) carries an additional G-C base pair in stem I and is flanked on each end by accessory sequences that are designed as short hairpins to reduce the occurance of inactive structures. **H3** (SEQ ID NO: 4) is an integrated hammerhead ribozyme that includes an RNA domain corresponding to a truncated version of an ATP- and adenosine-specific aptamer (35). **H4** and **H5** are modified versions of H3 that include an aptamer-domain mutation and a 3 base-pair extension of stem II, respectively. Arrowheads indicate the site of ribozyme-mediated cleavage.

Figure 6 shows evidence of ATP- and adenosine-mediated inhibition of a hammerhead ribozyme described in Example 1. (**A**) Hammerhead constructs **H1**, **H2** and **H3** (400 nM) were incubated with trace amounts of (5'-^{32}P)-labeled substrate (**S**) in the absence (–) or presence (+) of 1 mM ATP for 30 min. (**B**) The specificity of the effector molecule was examined by incubating **H3** and **S** for 45 min as described in Example 1 without (–) or with 1 mM of various nucleotides as indicated. Similarly, constructs **H4** and **H5** were examined for activity in the presence of 1 mM ATP. Reaction products were separated by a denaturing (8 M urea) 20% polyacrylamide gel and visualized by autoradiography. **E**, **S** and **P** identify enzyme, substrate and product bands, respectively.

Figure 7 plots kinetic analysis results of the catalytic inhibition of H3 by ATP described in Example 1. (**A**) Plot of H3 ribozyme activity (400 mM) in the presence of 10 μM (open circles) and 1 mM (filled circles) ATP. Dashed line

represents the average initial slope obtained in the absence of ATP or in the presence of as much as 1 mM dATP. **(B)** Plot of H3 ribozyme activity (k_{obs}) in the presence of various concentrations of dATP (open circles) and ATP (filled circles). Also plotted on the y axis are k_{obs} values for H1, H2 and H3 (open squares, filled squares and open circles, respectively) with no added effector molecules.

Figure 8 **(A)** depicts integrated constructs for allosteric induction by ATP (**H6**, SEQ ID NO: 5 and **H7**, SEQ ID NO: 6) and allosteric inhibition by theophilline (**H8**) described in Example 1. **H7** replaces the central U-A pair with a G.U mismatch and is designed to further reduce hammerhead catalysis. **H8** is analogous to H3 except that the ATP-aptamer domain is replaced by the theophylline aptamer corresponding to 'mTCT8-4' that was described by Jenison, *et al.* (21). Arrowhead indicates the site of ribozyme-mediated cleavage. **(B)** Induction of ribozyme catalysis during the course of a ribozyme reaction was examined by incubating H6 in the absence (open circles) and presence (open squares) of 1 mM ATP, and when ATP is added (filled circles), to a final concentration of 1 mM during an ongoing ribozyme reaction. Arrow indicates the time of ATP addition.

Figure 9 shows *in vitro* selection of self-cleaving DNAs described in Example 2. In a *a*, **(I)** a pool of 5′-biotinylated DNAs is immobilized on a streptavidin matrix, washed to remove unbound DNAs, then **(II)** eluted under the desired reaction conditions to separate self-cleaving DNAs from those that are inactive. **(III)** Selected DNAs are amplified by the polymerase chain reaction (PCR) and **(IV)** the selection round is completed by immobilizing the resulting double-stranded DNAs on new matrix followed by removal of the nonbiotinylated strand by chemical denaturation. **(V)** The pool is prepared for further analysis by PCR amplification with non-biotinylated primers. Encircled B indicates 5′ biotin. In *b*, the construct used for the initial round of selection contains a domain of 50 random-sequence nucleotides (N_{50}) flanked by 38 and 14 nucleotides of defined sequence. DNAs used in subsequent rounds carry an additional 26 nucleotides, as defined by primer 1 (SEQ ID NO: 7; primer 2 is SEQ ID NO: 8). Precursors that

cleave within the overlined region retain sufficient 5′ primer binding site for amplification and are expected to be favored during selection. In *c*, self-cleavage activity of the initial DNA pool (**G0**) and the pool isolated after seven rounds (**G7**) of selection. 5′ ^{32}P-labeled precursor DNA (**Pre**) was incubated in the presence (+) or absence (–) of 10 μM each of Cu^{2+} and ascorbate, or in the absence of Cu^{2+} or ascorbate (**–Cu^{2+}** and **–asc**, respectively) for various times as indicated. **M** is 5′ ^{32}P-labeled primer 3 and **Clv** identifies cleavage products.

Figure 10 shows sequence analysis and catalytic activity of individual G8 DNAs described in Example 2 (SEQ ID NOs: 9-31). In *a*, alignment of 34 sequences reveal the presence of two major classes of molecules that are characterized by sets of common sequences (boxed nucleotides). DNAs that were encountered more than once are identified by noting the number of occurrences in parentheses. In *b*, self-cleavage activity of ~5 nM 5′ ^{32}P-labeled precursor DNA from G8 DNA and from individuals CA1, CA2 and CA3 in the absence (-) or presence (+) of Cu^{2+} and ascorbate (10 μM each) are shown.

Figure 11 depicts cleavage site analysis of CA3 (lane 2), an optimized variant (variant 1, Figure 13b) of CA3 (lane 3) and CA1 (lane 4) described in Example 2. DNA size markers (lane 1) are 5′ ^{32}P-labeled DNAs of 10-13 nucleotides as indicated. The nucleotide sequence of these markers correspond to the 5′ terminal constant region of the precursor.

Figure 12 **(a)** shows an artificial phylogeny of CA1 (SEQ ID NO: 30) variants described in Example 2. The numbered sequence is wild-type CA1, and nucleotides of variants that differ from this sequence are aligned below. A dash indicates a deleted nucleotide. **(b)** Partial secondary-structure model for a variant of CA1 (arrowhead, SEQ ID NO: 32). Numbered nucleotides are derived from the region that was randomized in the starting pool. Asterisk indicates the primary cleavage site and the bar defines the region that undergoes detectable cleavage.

Not detailed are nucleotides within the 3′ primer binding site that are also required for catalytic activity.

Figure 13 shows a Cu^{2+}-dependent self-cleaving DNA described in Example 2. **(a)** Cleavage assay of G8 DNA, CA1 (SEQ ID NO: 30), CA3 (SEQ ID NO: 31) and the optimized population of CA3 variants was isolated after mutagenesis followed by five additional rounds of selection. **(b)** Sequence alignment of individual CA3 variants that have been optimized for catalytic function with Cu^{2+}. The numbered sequence is wild-type CA3, and nucleotides of variants that differ from this sequence are aligned below. A dash indicates a deleted nucleotide. Arrowheads identify CA3 variants 1-3 as denoted. Asterisk and bar indicate the major and minor Clv 2 cleavage sites, respectively.

Figure 14 shows the sequence and predicted secondary structures of minimized self-cleaving DNAs described in Example 3. (*A*) Sequence and secondary structure of a synthetic 69-nucleotide self-cleaving DNA that was isolated by *in vitro* selection (SEQ ID NO: 33). Numbers identify nucleotides that correspond to the 50-nucleotide random-sequence domain that was included in the original DNA pool (note that 19 bases of this domain have been deleted). The conserved nucleotides (11-31, boxed) are similar to those previously used to define this class of deoxyribozymes (Example 2). (*B*) A 46-nucleotide truncated version of class II DNAs that retains full activity (SEQ ID NO: 34). **I** and **II** designate stem-loop structures of the 46mer that are predicted by the structural folding program 'DNA mfold' (18, 19), and that were confirmed by subsequent mutational analysis (Figure 15). The conserved core of the deoxyribozyme spans nucleotides 27-46 and the major site of DNA cleavage is designated by the arrowhead. Encircled nucleotides can be removed to create a bimolecular complex where nucleotides 1-18 constitute the 'substrate' subdomain, and nucleotides 22-46 constitute the 'catalyst' subdomain.

Figure 15 shows a confirmation of stems I and II by mutational analysis described in Example 3. (*A*) Trace amounts of 5′ ^{32}P-labeled substrate DNAs (s1-s3) were incubated with 5 μM complementary or non-complementary catalyst DNAs (c1-c3) in reaction buffer A containing 10 μM $CuCl_2$ at 23°C for 15 min. Reaction products were separated by denaturing 20% polyacrylamide gel electrophoresis (PAGE) and imaged by autoradiography. Bracket identifies the position of the substrate cleavage products. (*B*) Self-cleavage activity of the original 46mer sequence compared to the activity of variant DNAs with base substitutions in stem II. Individual 46mer variants (100 pM 5′ ^{32}P-labeled precursor DNA) were incubated for the times indicated under reaction conditions as described above. Clv1 and Clv2 identify 5′-cleavage fragments produced upon precursor DNA (Pre) scission at the primary and secondary sites, respectively. Mutated positions are defined using the numbering system given in Figure 14.

Figure 16 identifies a triplex interaction between substrate and catalyst DNAs described in Example 3. A revised structural representation portrays a triple-helix interaction (dots) between the four base pairs of stem II and four consecutive pyrimidine residues near the 5′ end of the substrate DNA. c4 and s4 represent sequence variants of c3 (SEQ ID NO: 36) and s3 (SEQ ID NO: 35) that retain base pairing within stem II, and that use an alternate sequence of base triples. DNA cleavage assays were conducted as described in Figure 15*A*. Bracket identifies the position of the substrate cleavage products.

Figure 17 shows targeted cleavage of DNA substrates using deoxyribozymes with engineered duplex and triplex recognition elements. (*A*) A 101-nucleotide DNA incorporating three different deoxyribozyme cleavage sites was prepared by automated chemical synthesis (SEQ ID NO: 37). Each cleavage site consists of an identical leader sequence (shaded boxes) followed by a stem I recognition element of unique sequence. The specific base complementation between the synthetic catalyst DNAs c1, c3 and c7 are also depicted. The catalytic core sequences and the leader sequence/stem II interactions for each site are

identical (inset). Asterisks indicate G-T wobble pairs that allow cross reaction between c1 and the target for c3. Dots indicate base triple interactions. (*B*) Cleavage of the 101mer DNA by c1, c3, and c7 was examined by incubating trace amounts of 5′ ^{32}P-labeled substrate in reaction buffer containing 30 μM $CuCl_2$ at 23°C for 20 min., either in the absence (–) or presence of 5 μM catalyst DNA as indicated. Reaction products were separated by denaturing 10% PAGE and visualized by autoradiography. (*C*) Similarly, a 100-nucleotide DNA was prepared that contained three identical stem I pairing regions (shaded boxes) preceded by eight successive pyrimidine nucleotides of unique sequence (SEQ ID NO: 38). Three synthetic deoxyribozymes (c9, c10, c11) that carry identical stem I paring elements (inset) and extended stem II subdomains of unique sequence, were designed to target the three cleavage sites exclusively through DNA triplex interactions. (*D*) Cleavage of 100mer DNA by c9, c10, and c11 was established as described in (*B*) above. Miscleavage is detected for each triplex-guided deoxyribozyme upon extended exposure during autoradiography (*e.g.*, c11), indicating that weak-forming triplex interactions allow some DNA-cleavage activity to occur.

Figure 18 illustrates the *in vitro* selection of histidine-dependent deoxyribozymes described in Example 4. (**a**) A pool of 4 x 10^{13} biotin-modified DNAs was immobilized on a streptavidin-derivatized column matrix. Each DNA carries a single embedded RNA linkage (**rA**) and a 40-nucleotide random-sequence domain that is flanked by regions that are complementary to nucleotides that reside both 5′ and 3′ of the target phosphodiester (pairing elements *i* and *ii;* SEQ ID NOs: 39 and 40). These pre-engineered substrate-binding interactions are expected to increase the probability of isolating active catalysts (7). DNAs that catalyze the cleavage of the RNA linkage upon incubation with a solution buffered with histidine were released from the matrix, were amplified by the polymerase chain reaction (PCR), and the amplification products again were immobilized to complete the selection cycle (14-16). (**b**) Four classes of deoxyribozymes were determined by sequence comparison (SEQ ID NOs 41 to 44). Variants within each group differed by no more that two mutations from the sequences shown. Catalytic assays active (+)

when either HEPES or histidine buffers are used, while class II DNAs not active (–) when histidine is absent. Arrowhead identifies the site of cleavage and numbers correspond to the original 40-nucleotide random-sequence domain.

Figure 19 shows sequences and secondary structures of variant deoxyribozymes discussed in Example 4. (a) Individual DNAs isolated after reselection of mutagenized pools based on the class II deoxyribozyme (II) (SEQ ID NO: 45) or the HD2 deoxyribozyme (HD2 pool, SEQ ID NO: 46). Depicted are the nucleotide sequences for the mutagenized core of the parent DNAs and the nucleotide changes for each variant deoxyribozyme examined after reselection. Deoxyribozymes HD1 (SEQ ID NO: 47) and HD2 (SEQ ID NO: 48) were recovered from DNA pools generated after five rounds of reselection with 50 or 5 mM histidine, respectively. (b) Each deoxyribozyme was reorganized to create a bimolecular complex, whereby separate substrate molecules are recognized by two regions of base complementation (stems I and II) with the enzyme domain. Deoxyribozyme nucleotides are numbered consecutively from the 5′ terminus.

Figure 20 shows cofactor recognition by a deoxyribozyme described in Example 4. (a) Catalytic activity of HD1 with L-histidine, D-histidine, and various dipeptides that received (+) or did not receive (–) pretreatment with hydrochloric acid. HD1 (10 μM) was incubated in the presence of trace amounts of 5′ ^{32}P-labeled substrate oligonucleotide (Figure 19b) and were incubated at 23°C for 2.5 hr with 50 mM L-histidine, D-histidine, or various dipeptides as indicated. Reaction products were analyzed by denaturing (8 M urea) polyacrylamide gel electrophoresis (PAGE) and imaged by autoradiography. **S** and **P** identify substrate and product (5′-cleavage fragment) bands, respectively. (b) Chemical structures of L-histidine and the analogues used to probe deoxyribozyme cofactor specificity. (c) Representative deoxyribozyme assays for HD1 (E1) catalytic activity with selected amino acids and histidine analogues. Reactions and analyses were conducted as described in **a**.

Figure 21 are graphs showing the involvement of histidine in deoxyribozyme function described in Example 4. (a) Concentration-dependent induction of deoxyribozyme function by histidine. Open and shaded arrowheads indicate the concentration of histidine that was maintained during the selection of HD1 and HD2, respectively. (b) Dependence of deoxyribozyme function on pH. Data represented in the main plot was produced using 1 mM histidine while data given in the inset was obtained using 5 mM histidine. Data depicted with filled, open, and shaded circles was collected using MES–, Tris–, and CAPS–buffered solutions, respectively.

Detailed Description of the Invention

Natural ribozymes and artificial ribozymes and deoxyribozymes that have been isolated by *in vitro* selection are not known to operate as allosteric ribozymes. This invention is based upon the finding that small-molecule effectors can bind to ribozyme and deoxyribozyme domains and modulate catalytic rate. For example, using rational design strategies, a 'hammerhead' self-cleaving ribozyme described herein was coupled to different aptamer domains to produce ribozymes who's rates can be specifically controlled by adenosine and it's 5′-phosphorylated derivatives, or by theophilline. It is possible to construct, using a mix of *in vitro* selection and rational design strategies, novel biosensors that rely on nucleic acid sensor elements. To achieve this, unique RNA or DNA aptamers can be appended to ribozymes or deoxyribozymes, thereby creating new enzymes having catalytic rates that can be influenced by specific chemical effectors (*e.g.*, molecules of diagnostic interest), physical signals, and combinations thereof.

In the practice of the invention, purified functional DNA polynucleotides that exhibit allosteric properties that modify a function or configuration of the polynucleotide with a chemical effector, a physical signal, or combinations thereof, are constructed. In some embodiments, the DNA is an enzyme exhibiting allosteric

properties that modify the rate of catalysis of the enzyme. The invention further provides purified functional RNA or DNA polynucleotides having catalytic properties with rates that can be controlled by a chemical effector, a physical signal, or combinations thereof. In some embodiments, the polynucleotides contain from about 10 to about 100 bases; others are much larger.

Any element, ion, and/or molecule can be used as chemical effectors for interaction with the bioreactive allosteric polynucleotides of the invention. Examples include, but are not limited to, organic compounds and mixtures of organic compounds and metal ions. Chemical effectors may be amino acids, amino acid derivatives, peptides (including peptide hormones), polypeptides, nucleosides, nucleotides, steroids, sugars or other carbohydrates, pharmaceuticals, and mixtures of any of these. In many embodiments, the chemical effectors are microbial or cellular metabolites or other biological samples. Components found in liquid biological samples such blood, serum, urine, semen, tears, and biopsy homogenates taken from patients for medical or veterinary diagnostic or therapeutic purposes are particularly preferred chemical effectors in some embodiments. In industrial and environmental applications, the effectors are pesticides, herbicides, food toxins, product ingredients, reactants, and contaminants, drugs, and the like.

Bioreactive polynucleotides of the invention exhibit allosteric properties that modify polymer function or configuration with a physical signal or a combination of a physical signal and a chemical effector in alternate embodiments. Physical signals include, but are not limited to, radiation (particularly light), temperature changes, movement, physical conformational changes in samples, and combinations thereof.

Many embodiments employ bioreactive allosteric polynucleotides of the invention as biosensors in solution or suspension or attached to a solid support such as that illustrated in Figure 1. Alone or as a component of a biosensor, the polynucleotides are used to detect the presence or absence of a compound or its

concentration and/or a physical signal by contact with the polynucleotide. In a typical practice of these methods, a sample is incubated with the polynucleotide or biosensor comprising the polynucleotide as a sensing element for a time under conditions sufficient to observe a modification or configuration of the polynucleotide caused by the allosteric interaction. These are monitored using any method known to those skilled in the art, such as measurement and/or observation of polynucleotide self-cleavage; binding of a radioactive, fluorescent, or chromophoric tag; binding of a monoclonal or fusion phage antibody; or change in component concentration, spectrophotometric, or electrical properties. It is an advantage of the invention that current biosensor technology employing potentiometric electrodes, FETs, various probes, redox mediators, and the like can be adapted for use in conjunction with the new polynucleotide biosensors of the invention for measurement of changes in polynucleotide function or configuration.

The initial studies described in the Examples that follow have involved the creation and characterization of novel RNA- and DNA-cleaving enzymes that function with specific cofactors, or that can be regulated by specific small-molecule chemical effectors, physical signals, or combinations thereof. It is clear that additional molecules with similar sensor and biocatalytic properties can be created by similar means, thereby expanding the applications of such molecules. The creation and characterization of a prototype biosensor for ATP is given herein. One construct (H3) in particular shows ATP concentration-dependent catalytic activity, indicating that this ribozyme could be adapted for use in reporting the concentration of this ligand in test solutions. Specifically, H3 RNA actively self-cleaves in concentrations of ATP that are below 1 micromolar, but is maximally inhibited (170-fold rate reduction) in the presence of 1 millimolar ATP (Figure 3b). The catalytic rate of the ribozyme in concentrations of ATP that range between these two extremes is reflective of the ATP concentration, and can be used to determine unknown concentration values. It is important to note that the receptor portion of this allosteric ribozyme is completely artificial (created via *in vitro* selec-

tion) (35), and could be exchanged for other artificial or natural receptor domains that are specific for other ligands.

New and highly-specific receptors can be made via *in vitro* selection or 'SELEX' (4,5) using simple chromatographic and nucleic acid amplification techniques (4, and illustrated in the Examples). RNA and DNA 'aptamers' produced in this way can act as efficient and selective receptors for small organic compounds, metal ions, and even large proteins. In a dramatic display of RNA receptor function, a series of RNA aptamers for theophilline have been isolated (35) that show ~10,000-fold discrimination against caffeine, which differs from theophilline by a single methyl group.

One can isolate new classes of aptamers that are specific for innumerable compounds to create novel biosensors or even controllable therapeutic ribozymes for use in medical diagnostics, environmental analysis, *etc.* In the examples that follow, simple design strategies have been used to create conjoined aptamer-ribozyme complexes who's rates can be controlled by small effector molecules. Preliminary studies have already shown that theophilline-dependent ribozymes can be created through rational design. Theophilline, for example, is an important drug for the treatment of asthma and it's therapeutic effect is highly dependent on concentration. A biosensor for theophilline concentration would be of significant value. Further examination of this allosteric ribozyme and of other model ribozymes will help to lay the biochemical and structural foundations for the design of additional sensor molecules based on RNA and DNA.

It is an advantage of the invention that the discovery that DNA can function as an enzyme (5) has made practical the engineering of enzymes that are chemically more stable than either RNA or proteins. The half-life for the hydrolytic breakdown of a DNA phosphoester is ~200 million years, making DNA the most stable of the three major biopolymers. These features of DNA, coupled with the fact that DNA also can be made to bind various ligand with great specificity and

affinity, make this polymer an attractive medium for the creation of new industrial enzymes and as sensor elements for diagnostics. Also, modified DNAs can be made that are resistant to degradation by natural nucleases, making DNA analogues an attractive format for use in biological solutions. As illustrated hereafter, it has been found that DNA can be made to self-cleave in a metal ion-dependent fashion. The creation of these DNAs that catalyze their own cleavage in the presence of copper can now be used as a sensitive reporter of free copper concentration in solution. Another example given below is a polynucleotide reactive to histidine. Further engineering of such catalysts will yield allosteric DNA enzymes that can be used to detect a wide variety of ligands, or that report other reaction conditions such as the concentration of salts, pH, temperature, *etc.* In addition, these DNAs may be conducive to monitoring via amperometric H_2O_2 probes or by spectrophotometric analysis of the redox state of copper. Clearly, the diversity of signal read-out for both RNA and DNA sensors can be expanded.

Another feature of the invention is that use of polynucleotides as biosensors offer advantages over protein-based enzymes in a number of commercial and industrial processes. Problems such as protein stability, supply, substrate specificity and inflexible reaction conditions all limit the practical implementation of natural biocatalysts. As outlined above, however, DNA can be engineered to operate as a catalyst under defined reactions conditions. Moreover, catalysts made from DNA are expected to be much more stable and can be easily made by automated oligonucleotide synthesis. In addition, DNA catalysts are already selected for their ability to function on a solid support and are expected to retain their activity when immobilized.

The invention further encompasses the use of bioreactive allosteric polynucleotides attached to a solid support for use in catalytic processes. Immobilizing novel DNA enzymes will provide a new form of enzyme-coated surfaces for the efficient catalysis of chemical transformations in a continuous-flow reactor under both physiological and non-physiological conditions. The isolation of new DNA enzymes can be each tailor-made to efficiently catalyze specific chemical transformations under

user-defined reaction conditions. The function of catalytic DNAs to create enzyme-coated surfaces that can be used in various catalytic processes is described herein and illustrated in Figure 4. Due to the high stability of the DNA phosphodiester bond, such surfaces are expected to remain active for much longer than similar surfaces that are be coated with protein- or RNA-based enzymes.

A variety of different chromatographic resins and coupling methods can be employed to immobilize DNA enzymes. For example, a simple non-covalent method that takes advantage of the strong binding affinity of streptavidin for biotin to carry out a model experiment is illustrated in Figure 3. In other embodiments, DNA enzymes can be coupled to the column supports via covalent links to the matrix, thereby creating a longer-lived catalytic support. Various parameters of the system including temperature, reaction conditions, substrate and cofactor concentration, and flow rate can be adjusted to give optimal product yields. In fact, these parameters can be preset based on the kinetic characteristic that are displayed by the immobilized DNA enzyme. However, in practice, product formation will be monitored and the chromatographic parameters will be adjusted accordingly to optimize the system.

A prototype system for the large-scale processing of RNA substrates using an immobilized DNA enzyme is described herein. Product yields have been determined by analysis of ^{32}P-labeled substrate and product molecules by polyacrylamide gel electrophoresis of eluant samples. Multiple turn-over of immobilized enzyme during tests of the reactive chromatographic surface has been observed (Figure 4). The *in vitro* selection and engineering of new tailor-made DNA biocatalysts will produce catalytic surfaces for practical use and of unprecedented stability and catalytic versatility.

Examples

The following examples are presented to further illustrate and explain the present invention and should not be taken as limiting in any regard.

Example 1

As mentioned above, natural ribozymes (8) and ribozymes that have been isolated by *in vitro* selection are not known to operate as allosteric enzymes (6). This example illustrates allosteric ribozymes.

Using simple rational design concepts, aptamer domains with hammerhead self-cleaving ribozymes (13) were joined in a modular fashion, to create a series of catalytic RNAs that are amenable to both positive and negative allosteric control by small-molecule effectors. Initial efforts were focused on the 40-nucleotide ATP-binding aptamer, termed 'ATP-40-1', that was described by Sassanfar and Szostak (35). This motif shows a specific affinity for adenosine 5′ triphosphate (ATP; K_D ~10 μM) and adenosine, but has no detected affinity for a variety of ATP analogues including 2′-deoxyadenosine 5′ triphosphate (dATP) or the remaining three natural ribonucleoside triphosphates. The aptamer also undergoes a significant conformational change upon ligand binding, as determined by chemical probing studies. These characteristics were exploited to create a conjoined aptamer–ribozyme molecule that could be subject to ATP-dependent allosteric control.

The initial integrated design, H3, incorporates several key features into an otherwise unaltered bimolecular hammerhead ribozyme that is embodied by H1 (Figure 5). Each ribozyme and conjoined aptamer-ribozyme was prepared by *in vitro* transcription from a double-stranded DNA template that was produced by the polymerase chain reaction using the corresponding antisense DNA template and the primers 5′GAATTCTAATACGACTCACTATAGGCGAAAGCCGGGCGA (SEQ ID NO: 49) and 5′GAGCTCTCGCTACCGT (SEQ ID NO: 50). The former primer encodes the promoter for T7 RNA polymerase. 50-μl transcription reactions were performed by incubating of 30 pmoles template DNA in the presence of 50 mM Tris-HCl (pH 7.5 at 23°C), 15 mM $MgCl_2$, 5 mM dithiothreitol, 2 mM spermidine, 2 mM of each NTP, 20 μCi (α-^{32}P)-UTP and 600 units T7 RNA polymerase for 2 hr at 37°C. RNA products were separated by polyacrylamide gel electrophoresis

(PAGE), visualized by autoradiography and the ribozymes were recovered from excised gel slices by crush-soaking in 10 mM Tris-HCl (pH 7.5 at 23°C), 200 mM NaCl and 1 mM EDTA and quantified by liquid scintillation counting. The RNA substrate was prepared (Keck Biotechnology Resource Laboratory, Yale University) by standard solid-phase methods and the 2′-TBDMS group was removed by 24-hr treatment with triethylamine trihydrofluoride (15 µl per AU_{260} crude RNA). Substrate RNA was purified by PAGE, isolated by crush-soaking, (5′-^{32}P)-labeled with T4 polynucleotide kinase and (γ-^{32}P)-ATP, and repurified by PAGE. Even after exhaustive incubation with H1, approximately 45% of the RNA remains uncleaved. The kinetic calculations have been adjusted accordingly.

Superficially, sequences at the 5′ and 3′ termini were appended to make the constructs amenable to amplification by reverse transcription-polymerase chain reaction methods for future studies. Surveyed independently as H2 (Figure 5), these changes causes a 6-fold reduction in k_{obs} compared to H1 (rates are summarized in Table 1). In addition to the 5′-and 3′-terinal flanking sequences, H3 includes a modified hammerhead stem II that carries the ATP aptamer. The decision to locate the aptamer here was made primarily because changes in stem II can have large effects on the catalytic rates of hammerhead ribozymes (28). In the absence of ATP, this alteration causes an additional two-fold reduction in rate compared to H1.

The RNA-cleavage activity of H3 is significantly reduced when incubated with 1 mM ATP (Figure 6A). In contrast, ATP has no effect on the cleavage activity of H1 or H2. Moreover, inhibition is observed in the presence of adenosine, but not with dATP or the other ribonucleoside triphosphates (Fig 2B). This inhibition is highly specific and is consistent with the observed binding specificity of the aptamer (35).

Table 1. *Catalytic rates of various ribozyme constructs.* Constructs denoted with * and †, contain either a functional ATP aptamer or a defective ATP aptamer, respectively.

		k_{obs} (min^{-1})		
construct	stem II	none	ATP	dATP
H1	AAGGCC A IIIII AGCCGG	0.58	–	–
H2	AAGGCC A IIIII AGCCGG	0.10	–	–
H3*	CAAC IIII GUUG	0.054	0.00031	0.053
H4†	CAAC IIII GUUG	0.042	0.061	–
H5*	CAAGGCC IIIIIII GUUCCGG	0.075	0.13	–
H6*	CGUAUGC I•• I•• I GUGUGUG	0.022	0.12	0.027
H7*	CGUGUGC I••••• I GUGUGUG	0.0012	0.0098	0.0009

To investigate the mechanism of inhibition of H3 by ATP, two additional integrated constructs (Figure 5) were designed. H4 is identical to H3, but carries a G to C point mutation that is expected to eliminate ATP binding by the aptamer domain (35). As expected, this mutation eliminates the inhibitory effect of ATP. The allosteric effect may be due to the proximity of the aptamer and hammerhead domains. Specifically, structural models of the hammerhead indicate a parallel orientation for stems I and II (32). In the uncomplexed state, the aptamer domain is likely to exist in a single or a set of conformational state(s) that allow catalysis to proceed unhindered. However, when complexed with ATP, this domain undergoes a conformational change that presumably causes steric interference between structures that are appended to stems I and II. H5 carries an additional three base pairs in helix II, to further separate the domains, and is not inhibited by ATP. This

is consistent with an allosteric inhibition mechanism that involves conformational change and the mutually-exclusive formation of aptamer and ribozyme domains.

The inhibitory effect of ATP with H3 has been confirmed and quantitated by kinetic analysis. Ribozyme activity assays were conducted with trace amounts of substrate and excess ribozyme concentrations that significantly exceed K_m. Replicate k_{obs} values obtained for H1 and H2 at 200, 400 and 800 nM ribozyme concentration under identical assay conditions differed by less that two fold, suggesting that for each construct, k_{obs} values approach V_{max}. Reactions also contained 50 mM Tris–HCl (pH 7.5 at 23°C) and 20 mM $MgCl_2$, and were incubated at 23°C with concentrations of effector molecules and incubation times as noted for each experiments. Ribozyme and substrate were preincubated separately for ~10 min in reaction buffer and also with effector molecules when present, and reactions were initiated by combining preincubated mixtures. Assays with H8 were conducted in 50 mM HEPES (pH 7.3 at 23°C), 500 mM NaCl and 10 mM $MgCl_2$. Catalytic rates (k_{obs}) were obtained by plotting the fraction of substrate cleaved versus time and establishing the slope of the curve that represents the initial velocity of the reaction by a least-squares fit to the data. Kinetic assays were analyzed by PAGE and were visualized and analyzed on a Molecular Dynamics Phosphorimager. When shorter effector-molecule preincubations are used, the catalytic burst was more prominent and when encountered, a post-burst slope was used in the calculations. Replicate experiments routinely gave k_{obs} values that differed by less than 50% and the values reported are averages of two or more experiments. Equivalent rates were also obtained for duplicate ribozyme and substrate preparations.

The H3 ribozyme displays different cleavage rates, after a brief burst phase, with different concentrations of ATP (Figure 7A), with the curve closely predicting the K_D of the aptamer for its ligand. A plot of k_{obs} versus ATP or dATP concentration (Figure 7B) demonstrates that H3 undergoes ~170-fold reduction in catalytic rate with increasing concentrations of ATP, but is not inhibited by dATP.

Whether ATP could also be made to function as a positive effector of ribozyme function was investigated by designing H6 and subsequently H7 (Figure 8A), both which were found to display ATP-dependent allosteric induction. H6 is similar to H5, except that four Watson/Crick base-pairs in stem II are replaced with less-stable G.U mismatches. These changes are expected to significantly weaken stem II and result in diminished ribozyme activity. It was intended to exploit the fact that the G-C pair that begins stem II within the aptamer domain is not paired in the absence of ATP, but will form a stable pair when ATP is complexed (35), thereby increasing the overall stability of the stem and inducing catalytic activity. Indeed, a ~5-fold reduction in catalytic activity with H6 compared to H5 was found, yet ribozyme function could be specifically and fully recovered with ATP. The catalytic rate of H6 is also enhanced by ATP when added during the course of the reaction (Figure 8B).

As with allosteric effectors of proteins, there is no true similarity between the effector molecule and the substrate of the ribozyme. Substrate and effector occupy different binding sites, yet conformational changes upon effector binding result in functional changes in the neighboring catalytic domain. The specificity of allosteric control of ribozymes can be exquisite, and in this example the ribozyme activity is sensitive to the difference of a single oxygen atom in the effector molecule.

With similar model studies, a palate of design options and strategic approaches that can be used to create ribozymes with controlled catalytic activity can be built. The principles used here (secondary binding sites, conformational changes, steric effects and structural stabilization) as well as others may be generally applicable and can be used to design additional allosteric ribozymes, or even allosteric deoxyribozymes (37). For example, an allosteric hammerhead (H8, Figure 8A) that includes the theophylline aptamer described by Jenison, *et al.* (21) was designed. This construct displays a modest 3-fold reduction in ribozyme activity (k_{obs} of 0.006 v. 0.002 min^{-1}) when theophylline is added to a final concen-

tration of 100 μM. In addition, Sargueil, *et al.* (21) have suggested similar studies with the 'hairpin' self-cleaving ribozyme.

Example 2

The isolation by *in vitro* selection of two distinct classes of self-cleaving DNAs from a pool of random-sequence oligonucleotides are reported in this example. Individual catalysts from 'class I' require both Cu^{2+} and ascorbate to mediate oxidative self-cleavage. Individual catalysts from class II were found to operate with copper as the sole cofactor. Further optimization of a class II individual by *in vitro* selection yielded new catalytic DNAs that facilitate Cu^{2+}-dependent self-cleavage with rate a enhancement that exceed 1 million fold relative to the uncatalyzed rate of DNA cleavage.

DNA is more susceptible to scission via depurination/β-elimination or via oxidative mechanisms than by hydrolysis (27). To begin a comprehensive search for artificial DNA-cleaving DNA enzymes, DNAs that facilitate self-cleavage by a redox-dependent mechanism were screened for. Cleavage of DNA by chelates of redox-active metals (*e.g.*, Fe^{3+}, Cu^{2+}) in the presence of a reducing agent is expected to be a more facile alternative to DNA phosphoester hydrolysis due to the reactivity of hydroxyl radicals that are produced by reduction of H_2O_2 (*i.e.*, Fenton reaction). Moreover, a variety of natural and artificial 'chemical nucleases' rely on similar cleavage mechanisms (38-39).

Beginning with a pool of ~2 x 10^{13} random-sequence DNAs (Figure 13b), eight rounds of selection were carried out (5, 10) (see materials and methods section, below) for DNAs that self-cleave in the presence of $CuCl_2$ and ascorbate. The DNA pool that was isolated after seven rounds (G7 DNA) displays robust self-cleavage activity that requires both Cu^{2+} and ascorbate (Figure 13c). Trace amounts of non-specific DNA cleavage can be detected with Cu^{2+} and ascorbate concentrations of 100 μM or above, but no cleavage of random-sequence (G0)

DNA was detected under the final selection conditions (10 μM of each cofactor). In contrast, incubation of G7 DNA yields a number of distinct DNA cleavage products, suggesting that the pool contains multiple classes of DNAs that promote self-cleavage at unique sites.

Sequence analysis of individual DNAs from G8 reveals a diverse set of catalysts that were divided into two groups (Figure 10a) based on sequence similarities. Cleavage assays from three representative DNAs (CA1, CA2 and CA3) confirm that two distinct classes of catalysts have been isolated (Figure 10b). It was expected that the cleavage sites for the selected catalysts would reside exclusively within the first 23 nucleotides of the original construct (Figure 13b). Cleavage in this region would result in release of the molecule from the solid matrix, yet the cleaved molecules would retain enough of the original primer-binding site to allow amplification by PCR. Cleavage elsewhere in a molecule would release a DNA fragment that has lost the 5′-terminal primer-binding site, and would be incapable of significant amplification during PCR. Surprisingly, although CA1 promotes DNA cleavage within this expected region, CA2 and CA3 each cleave at a primary region (Clv 1) near the 5′ terminus as expected, and at a distal region (Clv 2) that resides within the domain that was randomized in the original DNA pool. The Clv 1/Clv 2 product ratio of CA3 is approximately 2:1.

The distribution of cleavage products between the two sites in CA3 is expected to result in a significant disadvantage during the selection process. About 35% of CA3-like molecules cleave within the center of the molecule (and hence are probably not amplified), while only about 65% cleave at the expected site and can be perpetuated in the next round of selection via amplification by PCR. In contrast, 100% of the catalysts that cleave exclusively in the primer-binding region can be amplified, giving individuals from class I an apparent selective advantage. However, CA3-like catalysts were found to persist in additional rounds of *in vitro* selection and actually come to dominate the population by generation 13. The success of these catalysts can be understood, in part, by examining the catalytic

rates of CA1 and CA3. The cleavage rate (k_{obs}) of 0.018 min^{-1} was obtained for CA1 under the final selection conditions, while cleavage at Clv 1 of CA3 occurs with a k_{obs} of 0.14 min^{-1}. Despite a high frequency of miscleavage, class II catalysts more rapidly cleave at the correct site, giving CA3-like catalysts a distinct selective advantage over catalysts from class I.

Cleavage sites for both classes have been further localized by gel-mobility analysis of the 5′ ^{32}P-labeled self-cleavage products (Figure 11). CA1 produces a major cleavage product with a gel mobility that corresponds to a 9-nucleotide fragment, and also yields a series of minor products that correspond to DNAs of 3 to 8 nucleotides. The cleavage site heterogeneity observed for CA1 is consistent with an oxidative cleavage mechanism that involves a diffusible hydroxyl radical. Typically, cleavage of nucleic acids by an oxidative cleaving agent occurs over a range of nucleotides, with a primary cleavage site flanked on each side by sites that are cleaved with decreasing frequency. It has been suggested that the frequency of DNA cleavage is proportional to the inverse of the distance that separates the target phosphoester linkage and the generation site of the hydroxyl radical (18). However, the distribution of cleavage products formed by CA1 are indicative of a unique active site that permits localized DNA cleavage to occur only at nucleotides that immediately flank the 5′ side of the major cleavage site.

Similarly, Clv 1 of CA3 consists of a series products that range in mobility from 9 to 14 nucleotides, with the major product corresponding to a 12-nucleotide DNA (Figure 11). The major product formed upon DNA scission at Clv 2 corresponds to 70 nucleotides, with minor products corresponding to DNAs of 66-69 nucleotides. The most frequent site of cleavage at Clv 2 is located near position 34 (G) of the original random-sequence domain. Oxidative cleavage of DNA can proceed by a variety of pathways, each that produce distinct cleavage-product termini (22). Therefore, conformation of these cleavage sites must now proceed by conducting a more detailed analysis of the chemical structures of the reaction products.

To gain insight into the secondary structure of CA1, an artificial phylogeny (2) of functional CA1 sequence variants for comparative sequence analysis (47) were produced. The 50 nucleotides that corresponds to the original random-sequence domain were mutagenized by preparing a synthetic DNA pool such that each wild-type nucleotide occurs with a probability of 0.85 and each remaining nucleotide occurs with a probability of 0.05. The resulting pool was subjected to five additional rounds of selection for activity in the presence of 10 μM each of Cu^{2+} and ascorbate. Sequence alignment of 39 resulting clones (Figure 12a) reveal two main regions (nucleotides 20-28 and 41-50) of strictly-conserved sequence interspersed with regions that tolerate variation. A total of 25 positions experienced two mutations or less. Other positions show sequence covariation, indicating that these nucleotides may make physical contact in the active conformation of the deoxyribozyme. For example, A32 and G40 frequently mutate to C or T, respectively. This suggests a preference for these bases to pair as C-G or A-T. Indeed, this inferred pairing occurs in a region (nucleotides 28-44) that has considerable base-pairing potential, consistent with the formation of a hairpin structure.

Using sequence data and truncation analyses, a partial secondary-structure model for CA1 was constructed (Figure 12b). Both the 5′- and 3′-terminal nucleotides show significant base-pairing potential with the substrate domain of the molecule. The putative hairpin domain described above (nucleotides 28-44) is flanked by the conserved 3′ terminus and by a highly-conserved region that is composed mainly of G residues. It was found that removal of an additional G-rich region that is located in the 3′ primer binding site abolishes the catalytic activity of CA1. Extended stretches of G residues that form 'G-quartet' structures (46) have been identified in a number of other single-stranded DNAs (3,20,26,48). The G-rich sequence in CA1 may also form a G-quartet, either independently or with other stretches of G residues that occur elsewhere in the primary structure of the catalyst.

CA1 has no detectable activity in the absence of ascorbate, but surprisingly, both the G8 population DNA and CA3 display significant cleavage when only Cu^{2+} is added (Figure 13a). A k_{obs} = 8 x 10^{-4} min^{-1} for Clv 1 was measured for CA3 in the presence of 10 μM Cu^{2+}. *In vitro* selection was employed to isolate CA3 variants with enhanced the Cu^{2+}-dep endent activity of CA3. CA3 was mutagenized (see above) and subjected to five rounds of selection using 10 μM Cu^{2+} as the sole cofactor. Sequence alignment of 40 resulting clones (Figure 13b) reveal a single region of highly-conserved sequence, spanning nucleotides 15 to 50 of the original random-sequence domain. The base identity of 27 nucleotides within this region were found to vary in three or fewer individuals. The most notable exceptions to this sequence conservation are a T deletion between nucleotides 39 and 45, and a T to G mutation that occurs at nucleotide 28. In a related selection experiment, active variants of CA3 in which nucleotides 1 through 20 of the original random-sequence domain have been deleted were isolated.

The catalytic activity of the reselected CA3 pool improved by nearly 100-fold, with variant DNAs 1, 2 and 3 (Figure 13b) displaying k_{obs} values of 0.052 min^{-1}, 0.033 min^{-1} and 0.043 min^{-1}, respectively. The uncatalyzed rate of DNA cleavage in the presence of Cu^{2+} was assessed by incubating 5′ ^{32}P-labeled DNA oligomer (primer 3) under identical conditions. No Cu^{2+}-dependent cleavage of DNA was detected, even after a 2-week incubation at 23°C. The overall rate enhancement of the CA3 variants was estimated to be considerably greater than 10^6 fold compared to the uncatalyzed rate. Both CA3 and variant 1 likely proceed via the same DNA cleavage mechanism, as evident by their similar catalytic cleavage patterns (Figure 11). A synthetic 87-nucleotide version of variant 1 that lacks the 3′-terminal primer-binding site remains active (k_{obs} = 0.02 min^{-1} for Clv 1, 10 μM Cu^{2+}), while an inhibitory effect is observed with 100 μM Cu^{2+}. In addition, the self-cleavage activity of this truncated DNA has a pH optimum of 7.5, with no specific monovalent cation requirement. Sequential deletion of nucleotides from the 5′ terminus of this DNA results in a progressive reduction in catalytic activity, with a 4-nucleotide deletion resulting in nearly complete loss of function.

The isolation of a variety of self-cleaving DNAs with Cu^{2+}/ascorbate-dependence is consistent with an earlier report (23) of site-specific cleavage of a single-stranded DNA under similar conditions. These results confirm that DNA is indeed capable of forming a variety of structures that promote chemical transformations. In addition, the catalytic rates for both classes of self-cleaving DNAs compare favorably to those attained by other deoxyribozymes and by natural and artificial ribozymes. The finding that DNA is also able to perform self-cleavage with Cu^{2+} alone is unexpected, since the mechanism for the oxidative cleavage of DNA also requires a reducing agent such as ascorbate or a thiol compound (38,39).

A number of chemical nucleases have been prepared by others and examined for their potential as site-specific DNA-cleaving agents. For example, 1,10-phenanthroline and similar agents bind DNA, presumably via intercalation, and positions copper ions near the ribose-phosphate backbone where formation of a reactive oxygen derivative favors cleavage of the DNA chain (39). Alternatively, metal-binding ligands have been attached to oligonucleotide probes, in order to construct highly-specific DNA cleaving agents that recognize DNA by triple-helix formation (26). The catalytic DNAs described in this report likely replace the role of chemical nucleases by forming their own metal-binding pockets so as to promote region-specific self-cleavage. In fact, the addition of 1,10-phenanthroline to a catalytic assay of a synthetic class II DNA actually inhibits catalytic function. The optimal Cu^{2+} concentration for the 87-nucleotide DNA is ~10 μM, with catalytic activity dropping significantly at both 1 and 100 μM Cu^{2+}. The inhibitory effect of 1,10-phenanthroline might be due to the reduction in concentration of free Cu^{2+} upon formation of Cu^{2+}-phenanthroline complexes.

While not wishing to be bound to any theory, several different mechanisms for the oxidative cleavage of class II DNAs seem possible. For example, the class II DNAs may simply scavenge for trace amounts of copper and reducing agents that are present in the reaction buffer. Alternatively, these DNA molecules might make use of an internal chemical moiety as the initial electron donor. In

each example, the catalytic DNAs could still cleave by an oxidative mechanism, but would at least appear to gain independence from an external source of reducing agent. The importance of H_2O_2 in oxidative processes can be examined with catalase, an enzyme that efficiently promotes the dismutation of H_2O_2 molecules to yield water and molecular oxygen. The catalytic activity of a representative DNA from class II is completely inhibited upon the addition of catalase, consistent with the notion that H_2O_2 is a necessary intermediate in an oxidative pathway for DNA cleavage. The catalytic rate of CA3 variants is greatly increased when incubated in the presence of added H_2O_2. For example, the 87-nucleotide DNA can be made to cleave quantitatively at Clv 1 (k_{obs} = 1.5 min^{-1}) in the presence of 10 μM Cu^{2+} and 35 mM H_2O_2.

It has not been determined whether trace amounts of H_2O_2 in water are used by the catalysts, or if the DNA can produce H_2O_2 in the absence of a reducing agent. It was found that preincubation of separate solutions of catalytic DNA in reaction buffer (minus Cu^{2+}) and of aqueous Cu^{2+}, followed by thermal denaturation of the catalase, results in full self-cleavage activity upon mixing of the two solutions. We also find that self-cleavage of the 87-nucleotide variant reaches a combined maximum (Clv 1 + Clv 2) of ~ 70%, regardless of the concentration of catalytic DNA present in the reaction. Similarly, preincubation of a reaction mixture with excess unlabeled catalyst (1 μM) followed by the addition of a trace amount of identical 5′ ^{32}P-labeled catalysts produces normal yields of labeled-DNA cleavage products. Finally, addition of fresh reaction buffer to a previously-incubated reaction mixture does not promote further DNA cleavage, as might be expected if limiting amounts of reducing agent were responsible for activity.

Certain constructs of the self-splicing ribozyme of *Tetrahymena* have been shown to catalyze the cleavage of DNA via a transesterification mechanism (19,33), and the ribozyme from RNase P has been found to cleave DNA by hydrolysis (31). Such ribozymes might also be made to serve as therapeutic DNA-cleaving agents, analogous to the function of RNA-cleaving 'catalytic antisense'

ribozymes (9). The secondary-structure model of CA1 (Figure 12b) includes stretches of predicted base pairing both 5′ and 3′ to the primary cleavage site, suggesting that 'substrate' and 'enzyme' domains can be separated. Likewise, preliminary analysis of class II molecules reveals similar base complementation. It is expected that both class I and class II DNAs can be engineered to create catalytic DNAs that specifically cleave DNA substrates with multiple turn-over kinetics.

In summary, two distinct classes of DNAs that promote their own cleavage have been isolated. One class requires copper and catalyzes the oxidative cleavage of DNA with a rate in excess of 1 million fold. Extensive regions of both classes of self-cleaving DNAs are important for the formation of catalytic structures, as implicated by sequence conservation found with selected individuals. These results support the view that DNA, despite the absence of ribose 2′-hydroxyl groups, has considerable potential to adopt higher-ordered structures with functions that are similar to ribozymes.

Materials and Methods

Oligonucleotides

All synthetic DNAs were prepared by automated chemical synthesis (Keck Biotechnology Resource Laboratory, Yale University). The starting pool is composed of DNAs that carry a 5′-terminal biotin moiety and a central domain of 50 random-sequence nucleotides. Primer 3 is an analogue of primer 1 (Figure 13b) that contains a 3′-terminal ribonucleoside. Primer 4 is the nonbiotinylated version of primer 2 (Figure 13b). Primer 5 is the 5′-biotinylated form of primer 1.

In vitro *selection*

A total of 40 pmoles of pool DNA in 40 µl buffer A (50 mM HEPES, pH 7.0 at 23°C, 0.5 M NaCl, 0.5 M KCl) was loaded on two streptavidin-matrix columns (Affinitip Strep20, Genosys Biotechnologies) and incubated for ~5 min.

Unbound DNAs were subsequently removed from each column by pre-elution with 500 µl of buffer A, then by 500 µl 0.2 N NaOH, and the resulting matrix-bound DNAs were equilibrated with 500 µl buffer A. Catalytic DNAs were eluted with three successive 20-µl aliquots of buffer B (buffer A, 100 µM $CuCl_2$, 100 µM ascorbate) for rounds 1-3, or buffer C (buffer A, 10 µM $CuCl_2$, 10 µM ascorbate) for rounds 4-8. Eluate from each column was combined with 120 µl 4 mM EDTA and 40 pmoles each of primers 1 and 2. Selected DNAs and added primers were recovered by precipitation with ethanol and amplified by PCR a 200 µl reaction containing 0.05 U µl-1 *Taq* polymerase, 50 mM KCl, 1.5 mM $MgCl_2$, 10 mM Tris-HCl (pH 8.3 at 23°C), 0.01 % gelatin, and 0.2 mM each dNTP for 25 cycles of 10 sec at 92°C, 10 sec at 50 °C and 30 sec at 72°C. The 5′-terminal region of each cleaved DNA, including the biotin moiety, was reintroduced at this stage. Subsequent rounds were performed by immobilizing 20 pmoles of pool DNA on a single streptavidin column and selected DNAs were amplified in a 100 µl reaction for 10 to 20 temperature cycles. Steps II-IV (Figure 13) were repeated until the population displayed the desired catalytic activity, at which time the pool was PCR amplified with primers 1 and 3, cloned (Original TA Cloning Kit, Invitrogen) and sequenced (Sequenase 2.0 DNA Sequencing Kit, U. S. Biochemicals). Reselections with CA1 and CA3 were initiated with 20 pmoles synthetic DNA. This is expected to offer near comprehensive representation of all sequence variants with seven or fewer mutations relative to wild type.

Catalytic assays

5′-^{32}P-labeled precursor DNA was prepared by PCR-amplifying double-stranded DNA populations or plasmid DNA using 5′-^{32}P-labeled primer 4 and either primer 5 or primer 3. The antisense strand is removed either by binding the biotinylated strand to a streptavidin matrix (primer 5) or by alkaline cleavage of the RNA phosphodiester-containing strand, followed by PAGE purification (primer 3). DNA self-cleavage assays (~5 nM 5′ ^{32}P-labeled precursor DNA) were conducted at 23°C in buffer A, with cofactors added as detailed for each experiment. For both *in vitro* selection and for assays, reaction buffers that contained ascorbate were

prepared just prior to use. Self-cleavage assays conducted with catalase (bovine liver, Sigma) contained 50 mM HEPES (pH 7.0 at 23°C), 50 mM NaCl, 10 μM $CuCl_2$, and 0.5 U/μl catalase, and were incubated at room temperature for 20 min. Catalase activity was destroyed by heating at 90°C for 5 min. Products were separated by denaturing (8 M urea) polyacrylamide gel electrophoresis (PAGE) using a 10% gel and visualized by autoradiography or visualized and quantitated by PhosphorImager (Molecular Dynamics).

Cleavage product analysis

Primary cleavage sites for CA1 and CA3 were identified by incubating 5′ ^{32}P-labeled precursor DNA in buffer C and assessing the gel mobility of the 5′-terminal cleavage fragments by analysis using a denaturing 20% PAGE as compared to a series of 5′ ^{32}P-labeled synthetic DNAs that correspond in sequence to the 5′ terminus of the precursor DNAs. Products resulting from sission at Clv 2 were analyzed by denaturing 6% PAGE.

Kinetic analysis

Catalytic rates were obtained by plotting the fraction of precursor DNA cleaved versus time and establishing the slope of the curve that represents the initial velocity of the reaction as determined by a least-squares fit to the data. Kinetic assays were conducted in buffer C or in buffer A plus 10 μM $CuCl_2$ as indicated for each experiment. Rates obtained from replicate experiments differed by less than two fold and the values reported are averages of at least two analyses.

Example 3

This example describes a DNA structure that can cleave single-stranded DNA substrates in the presence of ionic copper. This deoxyribozyme can self-cleave, or it can operate as a bimolecular complex that simultaneously makes use of duplex and triplex interactions to bind and cleave separate DNA substrates. DNA

strand scission proceeds with a k_{obs} of 0.2 min^{-1}, a rate that is ~10^{12}-fold faster than the uncatalyzed rate of DNA phosphoester hydrolysis. The duplex and triplex recognition domains can be altered, making possible the targeted cleavage of single-stranded DNAs with different nucleotide sequences. Several small synthetic DNAs were made to function as simple 'restriction enzymes' for the site-specific cleavage of single-stranded DNA.

A Minimal Cu^{2+}-Dependent Self-cleaving DNA. In Example 2, a variety of self-cleaving DNAs were isolated by *in vitro* selection from a pool of random-sequence DNAs. Most individual DNAs that were isolated after eight rounds (G8) of selection conformed to two distinct classes, based on similarities of nucleotide sequence and DNA cleavage patterns. Although individual DNAs from both class I and class II require Cu^{2+} and ascorbate for full activity, the G8 DNA population displays weak self-cleavage activity in the presence of Cu^{2+} alone. A representative class II DNA termed CA3 was further optimized for ascorbate-independent activity by applying *in vitro* selection to a DNA pool that was composed of mutagenized CA3 individuals. The sequence data from this artificial phylogeny of DNAs indicates that as many as 27 nucleotides, most of them located near the 3′ terminus of the molecule, are important for self-cleavage activity.

Beginning with the original G7 DNA population, an additional six rounds of *in vitro* selection was carried out for DNAs that self-cleave in the presence of 10 μM Cu^{2+}, without added reducing agent. Analysis of the G13 population of DNAs revealed robust self-cleavage activity, demonstrating that catalytic DNAs can promote efficient cleavage of DNA using only a divalent metal cofactor. The G13 population displays the same cleavage pattern that was observed with individual class II DNAs, indicating that class II-like DNAs dominate the final DNA pool.

A total of 27 individual DNAs from G13 were sequenced and, without exception, each carried a 21-nucleotide sequence domain that largely conformed to the consensus sequence that was used previously to define class II self-cleaving

DNAs. Although individuals that have a strictly conserved core (spanning nucleotides 11 to 31, Figure 14*A*) dominate the G13 pool, two common variations from this consensus sequence include a C to T mutation at position 17 (6 of 28 individuals) or the presence of six successive T's instead of five in the region spanning nucleotides 21 to 25 (4 of 27 individuals). However, significant differences in nucleotide sequence were found to occur outside this conserved domain, indicating that large portions of the class II deoxyribozymes isolated may not be necessary for catalytic activity. Indeed, three individual DNAs were found to have undergone deletions of 16, 19, and 20 nucleotides within the 50-nucleotide domain that was randomized in the original starting pool. The predicted secondary structure for the 19-nucleotide deletion mutant (69mer DNA, Figure 14*A*), obtained by the Zucker 'DNA mfold' program (33,50; the DNA mfold server can be accessed on the internet at www.ibc.wustl.edu/~zuker/dna/form1. cgi.), indicates the presence of three base-paired regions; two involve pairing between the original random-sequence domain and the 'substrate' domain, and one that involves putative base-pairing of nucleotides that lie within the conserved-sequence region. A synthetic DNA corresponding to the 69-mer depicted in Figure 14*A* undergoes Cu^{2+}-dependent self-cleavage at two locations with a combined catalytic rate of approximately 0.3 min^{-1} under the conditions used for *in vitro* selection (see Materials and Methods below for additional discussion on catalytic rates).

Whether the two pairing regions of the 69-mer that lie within the variable-sequence region could be replaced by a smaller stem-loop structure was tested by synthesizing a 46-mer DNA, in which 26 nucleotides of this imperfect hairpin were replaced by the trinucleotide loop GAA (Figure 14*B*). As expected, the truncated '46mer' DNA retains full catalytic activity, thereby confirming that the deleted nucleotides are not essential for deoxyribozyme function. This 46-nucleotide deoxyribozyme is predicted to adopt a pistol-like secondary structure (Figure 14*B*) composed of two base-paired structural elements (stems I and II) flanked by regions of single-stranded DNA. The primary site of DNA cleavage is located at position 14 which resides within one of the putative stem structures of

the 46mer. The catalyst also promotes DNA cleavage within a region located apart from the main cleavage site (Example 2), as might be expected for a deoxyribozyme that makes use of an oxidative cleavage mechanism (22).

Bimolecular Deoxyribozyme Complexes: Substrate Recognition by Duplex and Triplex Formation. Separate 'substrate' and 'catalyst' DNAs can be created from the 46mer by eliminating the connecting loop of stem I (Figure 14*B*). Active bimolecular complexes then can be reconstituted by combining independently prepared substrate and catalyst DNAs. Both the unimolecular 46mer and the bimolecular complexes examined cleave with identical rates, promoting primary-site cleavage with a k_{obs} of approximately 0.2 min^{-1}. The importance of stem I was confirmed (Figure 15*A*) by synthesizing different catalyst DNAs (c1, c2 and c3) and assessing their ability to cleave different substrate molecules (s1, s2 and s3). For example, c1 displays activity with its corresponding substrate (s1), but not when the non-complementary substrate DNAs s2 or s3 are substituted. Likewise, c2 and c3 only cleave their corresponding substrate DNAs s2 and s3, respectively. Extending stem I to create a more stable interaction was also found to confer greater binding affinity between substrate and catalyst oligonucleotides. These data indicate that base pairing interactions that constitute stem I are an essential determinant for catalyst/substrate recognition.

Stem II was examined by a similar approach using mutant versions of the 46mer self-cleaving DNA. A series of variant deoxyribozymes with one or two mutations included in the putative stem II structure were synthesized and assayed for catalytic activity (Figure 15*B*). Disruption of the original C35-G43 base pair in stem II, either by mutation of C to G at position 35 or mutation of G to C at position 43, results in a substantial loss of activity. Cleavage activity is partially restored when these mutations are combined in the same molecule to produce a G35-C43 base pair. These results are consistent with the stem-loop structure modeled in Figure 14. Additional support for the presence of stem II was found upon sequence analysis of the deoxyribozymes that are present in the original *in*

vitro-selected pool of DNAs. A single self-cleaving DNA was found with a core sequence that differs significantly from that of the most frequently represented deoxyribozyme. Nucleotides 38-40 of the more common 46mer sequence are replaced in the variant deoxyribozyme with the nucleotides 5′-CTGGGG. This alternative sequence extends stem II by a single C-G base pair, consistent with the formation of the predicted stem-loop structure.

Although the existence of stem II is supported by the data derived from mutational analysis, the fact that total restoration of deoxyribozyme activity was not achieved with restoration of base complementation indicates that the identities of the base pairs in this structural element are important for maximal catalytic function. Moreover, it was found that mutation or deletion of nucleotides 1-7 of the 46mer result in a dramatic loss of DNA cleavage activity. It was recognized that nucleotides 4-7 within this essential region of the substrate form a polypyrimidine tract that is complementary to the paired sequence of stem II for the formation of a YR*Y DNA triple helix (14).

To examine the possibility of triplex formation in the active structure of the deoxyribozyme, we modified both the base pairing sequence of stem II (c4) and the sequence of the polypyrimidine tract of the substrate (s4) to alter the specificity, yet retain the potential for forming four contiguous base triples (Figure 16). The c4 variant DNA cleaves its corresponding s4 DNA substrate, but shows no activity with a substrate that carries the original polypyrimidine sequence. It was found that even single mutations within stem II (*e.g.*, Figure 15*B*) or single mutations within the polypyrimidine tract cause significant reductions in catalytic activity. However, the introduction of six mutations in a manner that is consistent with triplex formation results in a variant (c4/s4) complex that displays full DNA cleavage activity. This is the first example of a catalytic polynucleotide, natural or artificial, that makes use of an extended triple helix for the formation of its active structure (43).

Targeted Cleavage of DNA 'Restriction Sites' with Deoxyribozymes. The results described above demonstrate that class II deoxyribozymes identify substrate DNAs by simultaneously utilizing two distinct recognition domains that are formed separately by stems I and II. These structures might be further exploited as recognition elements to engineer deoxyribozymes that selectively cleave DNAs at different target sites. To demonstrate this capability, a 101-nucleotide DNA that carries three identical leader sequences, each followed by different stem I recognition sequences was synthesized (Figure 17*A*). Three catalyst DNAs (c1, c3 and c7) each were designed to be uniquely complementary to one of the three target sites. When incubated separately with 101mer substrate, DNAs c3 and c7 cleave exclusively at their corresponding target sites, while c1 cleaves at its intended site and also to a lesser extent at the c3 cleavage site (Figure 17*B*). The cross reactivity observed with c1 can be explained by examining the base-pairing potential of stem I. Of the six nucleotides in the c1 recognition sequence, four can form standard base pairs, while the remaining two form G-T wobble pairs. The contribution of both duplex and triplex recognition elements presumably allows for detectable cleavage activity at this secondary location.

The triplex interaction that is defined by the base-pairing sequence of stem II can also be exploited to target specific DNA substrates. We designed three new catalyst DNAs (c9, c10 and c11) that carry identical stem I pairing subdomains, but that have expanded and unique stem II subdomains (Figure 17*C*). When incubated separately with a 100-nucleotide DNA that carries three uniquely complementary polypyrimidine tracts, each catalyst DNA cleaves its corresponding target site with a rate that corresponds well with that found for the original self-cleaving DNA. In this example, substrate selectivity is determined almost entirely by triplex formation, despite the presence of identical and extensive base complementation (stem I) between catalyst and substrate molecules.

Although DNA cleavage catalyzed by the deoxyribozyme is focused within the substrate domain, substantial (~30%) cleavage occurs within the con-

served core of the catalyst strand. This collateral damage causes inactivation of the deoxyribozyme and, as a result, super-stoichiometric amounts of catalyst DNA are needed to assure quantitative cleavage of DNA substrate. Cleavage of the substrate subdomain proceeds more rapidly than does cleavage within the catalytic core. In the presence of excess c1, s1 is cleaved at a rate of approximately 0.2 min^{-1} (reaction buffer containing 30 μM $CuCl_2$), reaching a plateau of ~80% cleaved after 20 min. In contrast, cleavage of c1 in the presence of excess s1 proceeds more than 2-fold slower, consistent with our earlier report that the ratio of self-cleavage localized in the substrate domain to self-cleavage in the catalytic core gives a ratio of ~2:1. It was established that, barring inactivation by miscleavage, the catalyst strand can undergo multiple turnover.

Cleaving Double-stranded DNA by Thermocycling. Class II catalyst DNAs are not able to cleave target DNAs when they reside within a duplex. The catalyst DNA, with its short recognition sequence, presumably cannot displace the longer and more tightly-bound complementary strand of the target in order to gain access to the cleavage site. It was found that an effective means for specific cleavage of one strand of an extended DNA duplex makes use of repetitive cycles of thermal denaturation and reannealing. For example, c3 remains inactive against a double-stranded DNA target in the absence of thermal cycling, but efficiently cleaves the same DNA substrate upon repeated heating and cooling cycles. Cleavage of the radiolabeled target is quantitative after 6 thermal cycles. DNA cleavage by class II DNAs occurs within the base-pairing region corresponding to stem I, presumably when this region is in double-helical form. This, coupled with the observation of substrate recognition by triplex formation, suggests that different DNA enzymes might be engineered to cleave duplex DNA substrates without the need for thermal denaturation. Such deoxyribozyme activity would be similar to that performed by a number of triplex-forming oligonucleotides that have been engineered to bind and cleave duplex DNA using a chemically-tethered metal complex such as Fe-EDTA (24-27).

Conclusions. In its unimolecular arrangement, the class II deoxyribozyme could be used to confer the capacity for self-destruction to an otherwise stable DNA construct. In its bimolecular form, the deoxyribozyme can act as an artificial restriction enzyme for single-stranded DNA, whereas protein-based nucleases that cleave non-duplex DNA do not demonstrate significant sequence specificity. It is likely that Ymaximal discrimination by class II catalysts between closely related target sequences can be achieved through careful design of the duplex and triplex recognition domains. This is expected to eliminate the cross reactivity that was observed here. Although the role of most nucleotides within the substrate domain are involved in substrate recognition, the importance of each nucleotide within the leader sequence has yet to be fully delineated. However, guided by the basic rules of duplex and triplex formation, one w3can now engineer highly-specific deoxyribozymes that can catalyze the cleavage of single-stranded DNA at defined locations along a polynucleotide chain.

Materials and Methods

Oligonucleotides

Synthetic DNAs were prepared by automated chemical synthesis (Keck Biotechnology Resource Laboratory, Yale University), and were purified by denaturing (8M urea) polyacrylamide gel electrophoresis (PAGE) prior to use. Double-stranded 101mer DNA was prepared by the polymerase chain reaction (PCR) as described in Example 2 using the primer DNAs 5′ ^{32}P-GTCGACCTGCG-AGCTCGA, (SEQ ID NO: 51) 5′GTAGATCGTAAAGCTTCG (SEQ ID NO: 52) and the 101mer DNA oligomer (Figure 17*A*) as template.

In vitro *selection*

Optimization of class II self-cleaving DNAs was achieved by *in vitro* selection essentially as described In Example 2 using a reaction mixture for DNA cleavage composed of 50 mM HEPES (pH 7.0 at 23°C), 0.5 M NaCl, 0.5 M KCl

(buffer A), and that included 10 μM $CuCl_2$. The selection process was initiated with 20 pmoles G7 PCR DNA in which the 5′ terminus of each catalyst strand carried a biotin moiety, thereby allowing DNA from this and subsequent generations to be immobilized on a streptavidin-derivatized chromatographic matrix. Reaction time was 15 min. for immobilized DNA from G8-G10 and 12, 7 and 5 min. for the G11-G13 DNA populations, respectively. Individual self-cleaving DNAs from G13 were analyzed by cloning (Original TA Cloning Kit, Invitrogen) and sequencing (Sequenase 2.0 DNA Sequencing Kit, U.S. Biochemicals).

DNA cleavage assays

To assess the DNA cleavage activity of self-cleaving molecules, radiolabeled precursor DNA was prepared by enzymatically tagging the 5′ terminus of synthetic DNAs in a reaction containing 25 mM CHES (pH 9.0 at 23°C), 5 mM $MgCl_2$, 3 mM DTT, 1 μM DNA, 1.2 μM (γ-^{32}P)-ATP (~130 μCi), and 1 U/μL T4 polynucleotide kinase, which was incubated at 37°C for 1 hr. The resulting 5′ ^{32}P-labeled DNA was isolated by denaturing PAGE and recovered from the gel matrix by crush-soaking in 10 mM Tris-HCl (pH 7.5 at 23°C), 0.2 M NaCl, and 1 mM EDTA. The recovered DNA was concentrated by precipitation with ethanol and resuspended in deionized water (Milli-Q, Millipore). Self-cleavage assays using trace amounts of radiolabeled precursor DNA (~100 pM) were conducted at 23°C in buffer A containing $CuCl_2$ as indicated for each experiment. Examinations of the DNA cleavage activity of bimolecular complexes were conducted under similar conditions using trace amounts of of 5′ ^{32}P-labeled 'substrate' DNA. Cleavage products were separated by denaturing PAGE, imaged by autoradiography or by PhosphorImager (Molecular Dynamics) and product yields were determined by quantitation (ImageQuant) of the corresponding precursor and product bands.

Kinetic analyses

Catalytic rates were estimated by plotting the fraction of precursor or substrate DNA cleaved versus time and establishing the slope of the curve that

represents the initial velocity of the reaction as determined by a least-squares fit to the data. Upon close examination, DNA cleavage in both the substrate and enzyme domains displayed a brief lag phase that complicates the determination of the initial cleavage rate. In order to avoid the lag phase, the initial slope was calculated only using data collected after the reaction had proceeded for 1 min. Rates obtained from replicate experiments differed by less than 50% and the values reported are averages of at least three analyses.

Example 4

The *in vitro* selection of a catalytic DNA that uses histidine as the active component for an RNA cleavage reaction is described in this example. An optimized deoxyribozyme only binds to L-histidine or to several closely-related analogues and subsequently catalyzes RNA phosphoester cleavage with a rate enhancement of ~10-million fold over the uncatalyzed rate. While not wishing to be bound to any theory, the DNA-histidine complex apparently performs a reaction that is analogous to the first step of the catalytic mechanism of RNase A, in which the imidazole group of histidine acts as a general base catalyst.

The class of deoxyribozymes that catalyze the cleavage of an RNA phosphoester bond using the amino acid histidine as a cofactor described herein is depicted in Figure 18a. To assure that metal-dependent deoxyribozymes were not recovered from the random-sequence pool of DNAs, the divalent metal-chelating agent ethylenedimainetetraacetic acid (EDTA) was included in a reaction mixture that was buffered with 50 mM histidine (pH 7.5). After 11 rounds of selective amplification, the DNA pool displayed RNA phosphoester-cleaving activity, both under *in vitro* selection conditions, and in a reaction buffer containing HEPES (50 mM, pH 7.5) in place of histidine. Individual molecules cloned from the final DNA pool were grouped into one of four sequence classes (Figure 19b), and representative clones were tested for catalytic activity. Only class II DNAs

demonstrate complete dependence on histidine while the remaining classes appear to operate independently of any metal ion or small organic cofactor.

The catalytic rate for the original class II deoxyribozyme was ~1000-fold slower (k_{obs} = 1.5 x 10^{-3} min^{-1}) than most natural self-cleaving ribozymes (44). As a result, further optimization of catalytic activity was sought in order to provide an artificial phylogeny of variant catalysts for comparative sequence analysis. A new DNA pool was prepared based on the sequence of class II deoxyribozymes, such that the 39 nucleotides corresponding to the original random-sequence domain were mutagenized with a degeneracy of 0.21 (6). Beginning with a mutagenized pool that sampled all possible variant DNAs with seven or fewer mutations relative to the original class II sequence, parallel reselection was conducted using reaction solutions buffered with either 50 mM histidine, or with 5 mM histidine and 50 mM HEPES. Individual DNAs isolated from the populations resulting from five rounds of reselection are more active than the original class II deoxyribozyme, and show specific patterns of conserved sequences and mutation acquisition (Figure 19a).

It was speculated that engineered pairing element *i* included in the original DNA construct (Figure 18a) was being utilized by class II deoxyribozymes. In contrast, it was recognized that a conserved-sequence domain near the 3′ end of the core (Figure 19a, nucleotides 32-36) was identical to pairing element *ii* . Considering these observations, individual deoxyribozymes HD1 and HD2 were designed to operate as separate substrate and enzyme domains (Figure 19b). Specificity for the substrate oligonucleotide is defined by the Watson/Crick base complementation between the substrate and the two pairing arms of the enzyme domain. Class II deoxyribozymes have an absolute requirement for histidine as show by the activity of the bimolecular HD1 construct to 'caged' histidine delivered in the form of dipeptides, and to free amino acids that were liberated from each dipeptide by acid hydrolysis (Figure 16a). In addition, HD1 accepts L-, but not D-histidine as a cofactor. However, samples of D-histidine become active upon

treatment with HCl in accordance with the accelerated rate of interconversion between the two isomeric forms in acidic conditions (11).

A larger panel of histidine analogues were examined (Fogire 16b) in order to more carefully examine the chemical groups of histidine that are important for catalytic activity and to rule out the possibility that catalysis might be due to a contamination of a metal ion cofactor. HD1 discriminates against a variety of histidine analogues, but shows full activity with the methyl ester of L-histidine (Figure 16c). Both the 1-methyl- and 3-methyl-L-histidine analogues do not support HD1 activity, indicating that the imidazole ring of histidine is important for deoxyribozyme function. As expected, HD2 has a similar pattern of cofactor discrimination (Table 2). Both catalysts show stereospecific recognition of histidine, and make use of interactions with the α-amino group, with both carboxyl oxygens, and with the imidazole group in order to attain maximize cofactor binding. Although a number of analogues cannot support deoxyribozyme activity, no compounds function as competitive inhibitors, indicating that their inactivity is due to the failure to bind the deoxyribozyme.

Table 2. *Relative k_{obs} values for HD2 in the presence of 25 mM L-histidine and various analogues (k_{obs} for L-histidine = 0.11 min^{-1}).*

cofactor	relative k_{obs}	fold discrimination
L-histidine	1	–
L-histidine methyl ester	0.93	1.1
L-histidine benzyl ester	0.76	1.3
α -methyl-DL-histidine	0.041	24
histidinamide	0.025	40
glycyl-histidine	0.006	170
histidinol	0.003	330
3-methyl-L-histidine	0.002	500
D-histidine	0.001	1000
1-methyl-L-histidine	$< 10^{-3}$	> 1000

The rate constant for HD2-promoted catalysis (k_{obs} of 0.2 min^{-1}, 50 mM histidine) is similar to that of natural self-cleaving ribozymes and corresponds to a rate enhancement of ~10 million fold over the uncatalyzed reaction ($k_{obs} < 10^{-8}$ min^{-1} under *in vitro* selection conditions). The dependence of the rate constant on histidine concentration is characteristic of the presence of a saturable binding site for histidine, although neither HD2 nor HD1 reach saturation even at 100 mM concentration of cofactor. The established specificity for particular cofactors, however, indicates that both catalysts do indeed form a histidine binding site. HD2 demonstrates greater activity with lower histidine concentrations, perhaps reflecting a greater binding affinity for histidine as would be expected due to its isolation from a low-histidine selection regiment.

The pH-dependent activity profile for HD2 also implicates histidine as an integral component of the catalytic process (Figure 21b). The rate constant of HD2 is entirely independent of pH between the values 7 and 9. However, the activity of this enzyme drops precipitously at pH values that lie outside this optimum range. Most revealing is the response of HD2 to low pH conditions. The k_{obs} values increase linearly with increasing pH between pH 4.5 and 5.5, giving a slope of approximately 1. This result is expected if the protonation state of a single functional group determined the catalytic rate. Moreover, a rate constant that is half the maximum value is obtained at pH 6, where this chemical group will be half deprotonated. This value corresponds precisely with the pK_a for the imidazole group of free histidine. Taken together, these results are consistent with a mechanism whereby the imidazole group serves as a general base catalyst for the deprotonation of the 2′-hydroxyl group, thereby activating the oxygen for nucleophilic attack on the neighboring phosphorus atom.

The loss of catalytic activity at higher pH values is not expected to be due to the protonation state of histidine, unless the pK_a of the imidazole group of a putative second histidine cofactor is dramatically shifted from its normal value. The β-amino group of histidine, which has a pK_a of greater than 9, conceivably could

be involved in catalysis as well. However, it is expected to find a loss of activity with pH values in excess of 9 or less than 4.5 due to the significant level of deprotonation of T and G residues or protonation of C and A residues, respectively.

Histidine was chosen as a candidate cofactor because of the potential for the imidazole side chain to function in both general acid and general base catalysis near neutral pH. This property is neither inherent to the four standard nucleotides of RNA nor to the remaining natural amino acids. As a consequence, histidine is one of the most-frequently used amino acids in the active sites of protein enzymes. For example, two active-site histidines are essential for the function of ribonuclease A from bovine pancreas, where both of these capacities are used to accelerate RNA cleavage. Although RNase A has long served as a model for the study of enzyme action, the specific roles that each active-site reside play in the catalytic process are still vigorously debated (31). The classical view holds that the histidine at position 12 acts as a general base for the deprotonation of the 2′ hydroxyl, while the histidine at position 119 acts as a general acid and protonates the 5′ oxyanion leaving group. Breslow and others (25,47) have proposed that the role for histidine 119 instead may be to protonate the phosphorane intermediate, thereby implicating general acid catalysis by the imidazole group as a priority step during the catalytic process. The data described herein indicate that the histidine cofactor for class II deoxyribozymes is not involved in a protonation step, but is functioning exclusively as a general base catalyst.

In comparison to proteins, the more repetitive nature of monomeric units that make up nucleic acids limits both the formation of fine structure in folded polynucleotides and the chemical reactivity of RNA and DNA. The fact that a nucleic acid enzyme can co-opt one of the favorite chemical units of protein-based enzymes supports the notion that RNA could rally its limited structure-forming potential and, using the catalytic tools of modern protein enzymes, could produce and maintain a complex metabolic state.

Materials and Methods

In vitro *selection and reselection*

In vitro selection was carried out essentially as described previously (5,7,47). The initial DNA pool was prepared by PCR amplification of the template 5′-CTAATACGACTCACTATAGGAAGAGATGGCGACATCTC$(N)_{40}$GTGAGGTTG-GTGTGGTTG (SEQ ID NOs: 53 and 54) (50 pmoles; N an equal probability of occurrence of the four nucleotides) in a 500-μL PCR reaction containing 400 pmoles of primer B2, 5′-biotin-GAATTCTAATACGACTCACTATrA (SEQ ID NO: 55), and 400 pmoles of primer 1, 5′-CAACC-ACACCAACCTCAC (SEQ ID NO: 56), with 4 thermocycles of 94°C (15 sec), 50°C (30 sec), and 72°C (30 sec). PCR reaction mixture was prepared as described previously (16). Amplified DNA was precipitated with ethanol, resuspended in binding buffer (50 mM HEPES (pH 7.5 at 23°C), 0.5 M NaCl, 0.5 M KCl, and 0.5 mM EDTA), and the solution was passed through a streptavidin-derivatized affinity matrix to generate immobilized single-stranded DNA[15]. The matrix displaying the pool DNA was repeatedly washed with binding buffer (1.5 mL over 30 min), and subsequently eluted over the course of 1 hr with three 20-μL aliquots of reaction buffer in which HEPES was replaced with 50 mM histidine (pH 7.5, 23°C). In rounds 8-11, reaction time was reduced to 25-15 min to favor those molecules that cleave more efficiently. Selected DNAs were preciptitated with ethanol and amplified by PCR using primer 1 and primer 2, 5′-GAATTCTA-ATACGACTCACTATAGGAAGAGATGGCGAC (SEQ ID NO: 57), and the resulting PCR was reamplified as described above to reintroduce the biotin and embedded ribonucleotide moieties.

Reselection of the class II deoxyribozyme was initiated with a pool of 10^{13} DNAs, each carrying a 39-nucleotide core that had been mutagenized with a degeneracy of 0.21 per position. Similarly, HD2 reselection was conducted with an initial pool in which 26 nucleotides was mutagenized to a degeneracy of 0.33 per position. Individual from the final selected pools were analyzed by cloning and sequencing. The DNA pools were prepared for this process by PCR amplification using primer 2 in place of primer B2. DNA populations and individual precursor DNAs were prepared for assays as described previously (7).

Deoxyribozyme Catalysis Assays

All catalytic assays were conducted in the presence of 0.5 M NaCl, 0.5 M KCl, 0.5 mM EDTA. Single turn-over assays contained a trace amount (~50 nM) substrate oligonucleotide and an excess (1-10 μM) DNA catalyst as described for each assay. The cofactor used was L-histidine unless otherwise stated. Reactions were terminated by addition to an equal volume of a solution containing 95% formamide, 0.05% xylene cyanol, and 0.05% bromophenyl blue and stored on ice prior to gel electrophoresis. Termination buffers containing both urea and EDTA were incapable of completely terminating deoxyribozyme activity.

Caged histidine experiments were conducted with intact dipeptides or with a concentration of hydrolyzed dipeptide products. Hydrolysis of dipeptides was achieved by incubating solutions containing 100 mM dipeptide and 6 N HCl in a sealed tube at 115°C for 23 hr. Samples were evaporated *in vacuo*, coevaporated with deionized water, and the resuspended samples were adjusted to neutral pH prior to use.

Catalytic rate constants (k_{obs}) either were determined by determining the initial velocity of the reaction (16) or by plotting the natural log of the fraction substrate remaining over time, where the negative slope of the line obtained over several half lives represents k_{obs}. The uncatalyzed rate was determined by incubating a trace amount of 5′ ^{32}P-labeled substrate under reaction conditions in the absence of deoxyribozyme at 23°C or at -20°C for 21 days. Comparative analysis of RNA phosphoester cleavage indicates that the rate constant for uncatalyzed RNA cleavage in the presence of histidine does not exceed the speed of substrate degradation due to radiolysis. It is expected that the maximum uncatalyzed rate for cleavage of the embedded RNA linkage does not exceed 10^{-8} min^{-1}. This value is ~10-fold lower than the value obtained in the presence of 1 mM Mg^{2+} (7).

The above description is for the purpose of teaching the person of ordinary skill in the art how to practice the present invention, and it is not intended to detail all those obvious modifications and variations of it which will become

apparent to the skilled worker upon reading the description. It is intended, however, that all such obvious modifications and variations be included within the scope of the present invention, which is defined by the following claims. The claims are intended to cover the claimed components and steps in any sequence which is effective to meet the objectives there intended, unless the context specifically indicates the contrary.

References

1. Beal, P. A. & Dervan, P. B. (1991) *Science* **251,** 1360-1363.

2. Berzal-Harranz, A., Joseph, A. and Burke, J. A. (1992) *Genes and Dev.* **6**, 129-134.

3. Bock, L. C., Griffin, L. C., Latham, J. A., Vermaas, E. H. and Toole, J. J. (1992) *Nature* **355**, 564-566.

4. Breaker, R.R. (1996) *Curr. Op. Biotech.* 7, 442-448.

5. Breaker, R.R., and Joyce, G.F. (1994) *Chem. & Biol.* **1**, 223-229.

6. Breaker, R.R., and Joyce, G.F. (1994) *Trends Biotech.* **12,** 268.

7. Breaker, R.R., and Joyce, G.F. (1995) *Chem. & Biol.* **2**, 665-660.

8. For reviews, see Cech, C.R. (1990) *Ann. Rev. Biochem.* **59,** 543; Symons, R.H. (1992) *Ann. Rev. Biochem.* **61,** 641; Altman, S., Kirsebom, L., and Talbot, S. (1995) In: *tRNA: Structure, Biosynthesis, and Function*, D. Söll and U. Raj Bhandary, eds., American Society for Microbiology, Washington, DC, pp 67-78; Michel F., and Ferat, J.-L. (1995) *Ann. Rev. Biochem.* **64,** 435 (1995).

9. Christoffersen, R. E. and Marr, J. J. (1995). *J. Med. Chem.* **38**, 2023-2037.

10. Cuenoud, B., and Szostak, J.W. (1995) *Nature* **375**, 611-614.

11. Engel, M.H. and Hare, P.E. (1982) *Carnegie Inst. Wash. Yearbook* **81**, 422-425.

12. Fedor, M.J. and Uhlenbeck, O.C. (1992) *Biochemistry* **31,** 12042.

13. Forster, A.C., and Symons, R.H. (1987) *Cell* **49,** 211.

14. Frank-Kamenetskii, M. D. and Mirkin, S. M. (1995) *Annu. Rev. Biochem.* **64,** 65-95.

15. Gilbert, W., (1986) *Nature* **319**, 618; Hirao, H. and Ellington, A.D., (1995) *Current Biol.* **5,** 1017.

16. Gold, L. (1995) *J. Biol. Chem.* **270,** 13581-13584.

17. Gold, L., Polisky, B., Uhlenbeck, O., Yarus, M. (1995) *Ann. Rev. Biochem.* **64**, 763-797.

18. Hermann, T. and Heumann, H. (1995) *RNA* **1**, 1009-1017.

19. Herschlag, D. & Cech, T. R. (1990) *Nature* **344**, 405-409.

20. Huizenga, D. E. and Szostak, J. W. (1995) *Biochemistry* **34**, 656-665.

21. Jenison, R.D., S. C. Gill, A. Pardi, B. Polisky, (1994) *Science* **263,** 1425.

22. Joshi, R. R., Likhite, S. M., Kumar, R. K. and Ganesh, K. N. (1994) *Biochim. Biophys. Acta* **1199**, 285-292.

23. Kazakov, S. A., Astashkina, T. G., Mamaev, S. V. and Vlassov, V. V. (1988). *Nature* **335**, 186-188.

24. Li, Y. and Sen, D. (1996) *Nature Struct. Biol.* **3**, 743-747

25. Lim, C. and Tole, P. (1992) *J. Am. Chem. Soc.* **114**, 7245-7252.

26. Lin, Y., Padmapriya, A., Morden, K. M. and Jayasena, S. D. (1995) *Proc. Natl. Acad. Sci. USA* **92**, 11044-11048.

27. Lindahl, T. (1993) *Nature* **362**, 709-715.

28. Long, D.M., and Uhlenbeck, O.C., (1994) *Proc. Natl. Acad. Sci. USA* **91,** 6977 and references therein; Tuschl, T., and Eckstein, F. (1993) *Proc. Natl. Acad. Sci. U.S.A.* **90**, 6991.

29. Moser, H. E. and Dervan, P. B. (1987) *Science* **238,** 645-650.

30. Perreault, J.-P. and Altman, S. (1992) *J. Mol. Biol.* **226**, 399-409.

31. Perreault, D.M. and Anslyn, E.V. (1997) *Angew. Chem. Int. Ed. Engl.* **36**, 432-450.

32. Pley, H.W., K. M. Flaherty, D. B. McKay, *Nature* **372,** 68 (1994); T. Tuschl, C. Gohlke, T. M. Jovin, E. Westhof, F. Eckstein, Science 266,785 (1994); S. T. Sigurdsson and F. Eckstein, *Trends Biotech.* **13,** 286 (1995); W. G. Scott, J. T. Finch, A. Klug, *Cell* **81,** 991 (1995).

33. Robertson, D. L. and Joyce, G. F. (1990) *Nature* **344,** 467-468.

34. SantaLucia Jr., J., Allawi, H. T. and Seneviratne, P. A. (1996) *Biochemistry* **35,** 3555-3562.

35. Sassanfar, M., and Szostak, J.W. (1993) *Nature* **364,** 550-553 and *Science* **263,** 1425-1429.

36. Schultz, P.G., Lerner, R.A. (1995) *Science* **252,** 1835-1842.

37. Serra, M.J., and Turner, D.H. (1995) *Methods Enzymol.* **259,** 242.

38. Sigman, D. S. & Chen, C. B. (1990) *Ann. Rev. Biochem.* **59,** 207-236.

39. Sigman, D. S., Mazumder, A. & Perrin, D. M. (1993) *Chem. Rev.* **93,** 2295-2316.

40. Strobel, S. A. and Dervan, P. B. (1990) *Science* **249,** 73-75.

41. Strobel, S. A. and Dervan, P. B. (1991) *Nature* **350,** 172-174.

42. Strobel, S. A. and Dervan, P. B. (1992) *Methods Enzymol.* **216,** 309-321.

43. Strobel, S. A. and Doudna, J. A. (1997) *Trends Biochem. Sci.* **22,** 262-266.

44. Symons, R.H. (1992) *Ann. Rev. Biochem.* **61,** 641-671.

45. Walsh, C. (1978) *Enzyme Reaction Mechanisms*, W. H. Freeman and Co., New York.

46. Williamson, J.R. (1994) *Ann. Rev. Biophys. Biomol. Struct.* **23,** 703-730.

47. Wladkowski, B.D., Krauss, M. & Stevens, W.J. (1995) *J. Am. Chem. Soc.* **117,** 10537-10545.

48. Woese, C. R. & Pace, N. R. (1993) In: *The RNA World*, R. R. Gesteland and J. F. Atkins, eds. Cold Spring Harbor Laboratory Press pp 91-117.

49. Wyatt, J. R., Vickers, T. A., Robertson, J. L., Buckheit, J., R. W., Klimkait, T., DeBaets, E., Davis, P. W., Rayner, B., Imbach, J. L. & Ecker, D. J. (1994) *Proc. Natl. Acad. Sci. USA* **91**, 1356-1360.

50. Zuker, M. (1989) *Science* **244**, 48-52.

The papers cited herein are expressly incorporated in their entireties by reference.

SEQUENCE LISTING

(1) GENERAL INFORMATION:

(i) APPLICANT: Ronald R. Breaker

(ii) TITLE OF INVENTION: Bioreactive Allosteric Polynucleotides

(iii) NUMBER OF SEQUENCES: 57

(iv) CORRESPONDENCE ADDRESS:
(A) ADDRESS: Yale University Biology Department
(B) STREET: 219 Prospect Street
(C) CITY: New Haven
(D) STATE: Connecticut
(E) COUNTRY: United States of America
(F) ZIP CODE: 06520-8103

(v) COMPUTER READABLE FORM:
(A) MEDIUM TYPE: 3.5" 1.44 Mb diskette
(B) COMPUTER: IBM PC
(C) OPERATING SYSTEM: MS DOS
(D) SOFTWARE: Word Processing

(vi) CURRENT APPLICATION DATA:
(A) APPLICATION NUMBER:
(B) FILING DATE:
(D) CLASSIFICATION:

(vii) PRIOR APPLICATION DATA:
(A) APPLICATION NUMBER: 60/033,684
(B) FILING DATE: 19-DEC-1996

(viii) ATTORNEY INFORMATION:
(A) NAME: Mary M. Krinsky
(B) REGISTRATION NO.: 32423
(C) REFERENCE/DOCKET NUMBER: OCR-794

(ix) TELECOMMUNICATION INFORMATION:
(A) TELEPHONE NUMBER: 203-773-9544
(B) TELEFAX NUMBER: 203-772-0587

(2) INFORMATION FOR SEQ ID NO: 1:

(i) SEQUENCE CHARACTERISTICS:
(A) LENGTH: 46
(B) TYPE: nucleic acid
(C) STRANDEDNESS: single
(D) TOPOLOGY: linear

(ii) MOLECULE TYPE:
(A) DESCRIPTION: DNA

(ix) FEATURE:
(A) NAME/KEY: self-cleaving DNA

(xi) SEQUENCE DESCRIPTION: SEQ ID NO: 1:

GAATTCTAAT ACGACTCAAA GTGAGTCTGG GCCTCTTTTT AAGAAC 46

(3) INFORMATION FOR SEQ ID NO: 2:

(i) SEQUENCE CHARACTERISTICS:
(A) LENGTH: 34
(B) TYPE: nucleic acid
(C) STRANDEDNESS: single
(D) TOPOLOGY: linear

(ii) MOLECULE TYPE:
(A) DESCRIPTION: RNA

(ix) FEATURE:
(A) NAME/KEY: H1 ribozyme

(xi) SEQUENCE DESCRIPTION: SEQ ID NO: 2:

GGCGACCCUG AUGAGGCCGA AAGGCCGAAA CGGU 34

(4) INFORMATION FOR SEQ ID NO: 3:

(i) SEQUENCE CHARACTERISTICS:
(A) LENGTH: 56
(B) TYPE: nucleic acid
(C) STRANDEDNESS: single
(D) TOPOLOGY: linear

(ii) MOLECULE TYPE:
(A) DESCRIPTION: RNA

(ix) FEATURE:
(A) NAME/KEY: H2 ribozyme

(xi) SEQUENCE DESCRIPTION: SEQ ID NO: 3:

GGCGAAAGCC GGGCGACCCU GAUGAGGCCG AAAGGCCGAA ACGGUAGCGA GAGCUC 56

(5) INFORMATION FOR SEQ ID NO: 4:

(i) SEQUENCE CHARACTERISTICS:
(A) LENGTH: 80
(B) TYPE: nucleic acid

(C) STRANDEDNESS: single
(D) TOPOLOGY: linear

(ii) MOLECULE TYPE:
(A) DESCRIPTION: RNA

(ix) FEATURE:
(A) NAME/KEY: H3 ribozyme

(xi) SEQUENCE DESCRIPTION: SEQ ID NO: 4:

GGCGAAAGCC GGGCGACCCU GAUGAGUUGG GAAGAAACUG UGGCACUUCG 50

GUGCCAGCAA CGAAACGGUA GCGAGAGCUC 80

(6) INFORMATION FOR SEQ ID NO: 5:

(i) SEQUENCE CHARACTERISTICS:
(A) LENGTH: 89
(B) TYPE: nucleic acid
(C) STRANDEDNESS: single
(D) TOPOLOGY: linear

(ii) MOLECULE TYPE:
(A) DESCRIPTION: RNA

(ix) FEATURE:
(A) NAME/KEY: H6 ribozyme

(xi) SEQUENCE DESCRIPTION: SEQ ID NO: 5:

GGCGAAAGCC GGGCGACCCU GAUGAUGAGU GUGUGGGAAG AAACUGUGGC 50

ACUUCGGUGC CAGCGUAUGC GAAACGGUAG CGAGAGCUC 89

(7) INFORMATION FOR SEQ ID NO: 6:

(i) SEQUENCE CHARACTERISTICS:
(A) LENGTH: 77
(B) TYPE: nucleic acid
(C) STRANDEDNESS: single
(D) TOPOLOGY: linear

(ii) MOLECULE TYPE:
(A) DESCRIPTION: RNA

(ix) FEATURE:
(A) NAME/KEY: H8 ribozyme

(xi) SEQUENCE DESCRIPTION: SEQ ID NO: 6:

GAAAGCCGGG CGACCCUGAU GAGUUGAUAC CAGCACUUCG GUGCCCUUGG 50

CAGCAACGAA ACGGGUAGCG AGAGCUC 77

(8) INFORMATION FOR SEQ ID NO: 7:

(i) SEQUENCE CHARACTERISTICS:
(A) LENGTH: 35
(B) TYPE: nucleic acid
(C) STRANDEDNESS: single
(D) TOPOLOGY: linear

(ii) MOLECULE TYPE:
(A) DESCRIPTION: DNA

(ix) FEATURE:
(A) NAME/KEY: primer 1

(xi) SEQUENCE DESCRIPTION: SEQ ID NO: 7:

GTTTCGCATT GGACTAAGTC CCAACCACAC CAACC 35

(9) INFORMATION FOR SEQ ID NO: 8:

(i) SEQUENCE CHARACTERISTICS:
(A) LENGTH: 38
(B) TYPE: nucleic acid
(C) STRANDEDNESS: single
(D) TOPOLOGY: linear

(ii) MOLECULE TYPE:
(A) DESCRIPTION: DNA

(ix) FEATURE:
(A) NAME/KEY: primer 2

(xi) SEQUENCE DESCRIPTION: SEQ ID NO: 8:

GAATTCTAAT ACGACTCACT ATAGGAAGAG ATGGCGAC 38

(10) INFORMATION FOR SEQ ID NO: 9:

(i) SEQUENCE CHARACTERISTICS:
(A) LENGTH: 49
(B) TYPE: nucleic acid
(C) STRANDEDNESS: single
(D) TOPOLOGY: linear

(ii) MOLECULE TYPE:
(A) DESCRIPTION: DNA

(ix) FEATURE:
(A) NAME/KEY: G8 DNA

(xi) SEQUENCE DESCRIPTION: SEQ ID NO: 9:

GCAGCCAAGG GTAGGAGCTG GAGGATGACA GGCGGGGTGA TAACTAGAA 49

(11) INFORMATION FOR SEQ ID NO: 10:

(i) SEQUENCE CHARACTERISTICS:
(A) LENGTH: 50
(B) TYPE: nucleic acid
(C) STRANDEDNESS: single
(D) TOPOLOGY: linear

(ii) MOLECULE TYPE:
(A) DESCRIPTION: DNA

(ix) FEATURE:
(A) NAME/KEY: G8 DNA

(xi) SEQUENCE DESCRIPTION: SEQ ID NO: 10:

TTATATAGTC GAGTCCATTC GAGGTAGGCG GGAACGGTAC TGGTAGAAG 50

(12) INFORMATION FOR SEQ ID NO: 11:

(i) SEQUENCE CHARACTERISTICS:
(A) LENGTH: 52
(B) TYPE: nucleic acid
(C) STRANDEDNESS: single
(D) TOPOLOGY: linear

(ii) MOLECULE TYPE:
(A) DESCRIPTION: DNA

(ix) FEATURE:
(A) NAME/KEY: G8 DNA

(xi) SEQUENCE DESCRIPTION: SEQ ID NO: 11:

TCTCACGTCA GGAGGGTAGA CTGGTAGCGAT AGGCGGCGG GGTGTAACAG AA 52

(13) INFORMATION FOR SEQ ID NO: 12:

(i) SEQUENCE CHARACTERISTICS:
(A) LENGTH: 50
(B) TYPE: nucleic acid
(C) STRANDEDNESS: single
(D) TOPOLOGY: linear

(ii) MOLECULE TYPE:

(A) DESCRIPTION: DNA

(ix) FEATURE:
(A) NAME/KEY: G8 DNA

(xi) SEQUENCE DESCRIPTION: SEQ ID NO: 12:

AGAGCTGTGG ATCTGGAGCA AGGAAATCTCG GTAGGCGGG TTTACTAGAA 50

(14) INFORMATION FOR SEQ ID NO: 13:

(i) SEQUENCE CHARACTERISTICS:
(A) LENGTH: 48
(B) TYPE: nucleic acid
(C) STRANDEDNESS: single
(D) TOPOLOGY: linear

(ii) MOLECULE TYPE:
(A) DESCRIPTION: DNA

(ix) FEATURE:
(A) NAME/KEY: G8 DNA

(xi) SEQUENCE DESCRIPTION: SEQ ID NO: 13:

GCCAGAACCT CCGTAGGCGG AAATGAGTAAA CATTGTAGA AGAGGGGG 48

(15) INFORMATION FOR SEQ ID NO: 14:

(i) SEQUENCE CHARACTERISTICS:
(A) LENGTH: 45
(B) TYPE: nucleic acid
(C) STRANDEDNESS: single
(D) TOPOLOGY: linear

(ii) MOLECULE TYPE:
(A) DESCRIPTION: DNA

(ix) FEATURE:
(A) NAME/KEY: G8 DNA

(xi) SEQUENCE DESCRIPTION: SEQ ID NO: 14

GTTAGAACCTC GTAGGCGGA AATGAGTAAAC ATGTAGAAG AGGGG 45

(16) INFORMATION FOR SEQ ID NO: 15:

(i) SEQUENCE CHARACTERISTICS:
(A) LENGTH: 50
(B) TYPE: nucleic acid
(C) STRANDEDNESS: single
(D) TOPOLOGY: linear

(ii) MOLECULE TYPE:
(A) DESCRIPTION: DNA

(ix) FEATURE:
(A) NAME/KEY: G8 DNA

(xi) SEQUENCE DESCRIPTION: SEQ ID NO: 15:

GTTTGAGGGA GACAGATGTG GAAGGCGGGGA GATTGATTC TCTAGAAGGT 50

(17) INFORMATION FOR SEQ ID NO: 16:

(i) SEQUENCE CHARACTERISTICS:
(A) LENGTH: 40
(B) TYPE: nucleic acid
(C) STRANDEDNESS: single
(D) TOPOLOGY: linear

(ii) MOLECULE TYPE:
(A) DESCRIPTION: DNA

(ix) FEATURE:
(A) NAME/KEY: G8 DNA

(xi) SEQUENCE DESCRIPTION: SEQ ID NO: 16:

AGGTAGGCGG GGAATACTAA CGCTGTTCAGT ATTATAGAA 40

(18) INFORMATION FOR SEQ ID NO: 17:

(i) SEQUENCE CHARACTERISTICS:
(A) LENGTH: 48
(B) TYPE: nucleic acid
(C) STRANDEDNESS: single
(D) TOPOLOGY: linear

(ii) MOLECULE TYPE:
(A) DESCRIPTION: DNA

(ix) FEATURE:
(A) NAME/KEY: G8 DNA

(xi) SEQUENCE DESCRIPTION: SEQ ID NO: 17:

GTATGGGGTA TATCTGAAGG CGGAAATAGCT ATTGGGCTG TTGTAGAA 48

(19) INFORMATION FOR SEQ ID NO: 18:

(i) SEQUENCE CHARACTERISTICS:
(A) LENGTH: 50
(B) TYPE: nucleic acid

(C) STRANDEDNESS: single
(D) TOPOLOGY: linear

(ii) MOLECULE TYPE:
(A) DESCRIPTION: DNA

(ix) FEATURE:
(A) NAME/KEY: G8 DNA

(xi) SEQUENCE DESCRIPTION: SEQ ID NO: 18:

AGCAATTCTA GGATAGGCGG GAAAGTGGAAT ATGCGTTTC AGTTGTAGAA 50

(20) INFORMATION FOR SEQ ID NO: 19:

(i) SEQUENCE CHARACTERISTICS:
(A) LENGTH: 48
(B) TYPE: nucleic acid
(C) STRANDEDNESS: single
(D) TOPOLOGY: linear

(ii) MOLECULE TYPE:
(A) DESCRIPTION: DNA

(ix) FEATURE:
(A) NAME/KEY: G8 DNA

(xi) SEQUENCE DESCRIPTION: SEQ ID NO: 19:

ATTATGGAAG ACAGATGAGG GCAGGCGGGAA TATACACAT ATTAAGAA 48

(21) INFORMATION FOR SEQ ID NO: 20:

(i) SEQUENCE CHARACTERISTICS:
(A) LENGTH: 43
(B) TYPE: nucleic acid
(C) STRANDEDNESS: single
(D) TOPOLOGY: linear

(ii) MOLECULE TYPE:
(A) DESCRIPTION: DNA

(ix) FEATURE:
(A) NAME/KEY: G8 DNA

(xi) SEQUENCE DESCRIPTION: SEQ ID NO: 20:

TGATAGGCGG CTAACCCTGC TTACGGGTTAT GGTTAGTTA GAA 43

(22) INFORMATION FOR SEQ ID NO: 21:

(i) SEQUENCE CHARACTERISTICS:

(A) LENGTH: 43
(B) TYPE: nucleic acid
(C) STRANDEDNESS: single
(D) TOPOLOGY: linear

(ii) MOLECULE TYPE:
(A) DESCRIPTION: DNA

(ix) FEATURE:
(A) NAME/KEY: G8 DNA

(xi) SEQUENCE DESCRIPTION: SEQ ID NO: 21:

TGATAGGCGG GCTAACCTGC CTTCGGGTTAT GGTTAGTTA GAA 43

(23) INFORMATION FOR SEQ ID NO: 22:

(i) SEQUENCE CHARACTERISTICS:
(A) LENGTH: 46
(B) TYPE: nucleic acid
(C) STRANDEDNESS: single
(D) TOPOLOGY: linear

(ii) MOLECULE TYPE:
(A) DESCRIPTION: DNA

(ix) FEATURE:
(A) NAME/KEY: G8 DNA

(xi) SEQUENCE DESCRIPTION: SEQ ID NO: 22:

GTATAGTGAT CTCGGGTCTC TGTCTATGAAG AACTGTAGC CATAAT 46

(24) INFORMATION FOR SEQ ID NO: 23:

(i) SEQUENCE CHARACTERISTICS:
(A) LENGTH: 44
(B) TYPE: nucleic acid
(C) STRANDEDNESS: single
(D) TOPOLOGY: linear

(ii) MOLECULE TYPE:
(A) DESCRIPTION: DNA

(ix) FEATURE:
(A) NAME/KEY: G8 DNA

(xi) SEQUENCE DESCRIPTION: SEQ ID NO: 23:

GTATAGTGAT CTGGGGTCTG TCTATGAAGAA CTGTAGCCA TAAT 44

(25) INFORMATION FOR SEQ ID NO: 24:

(i) SEQUENCE CHARACTERISTICS:
(A) LENGTH: 50
(B) TYPE: nucleic acid
(C) STRANDEDNESS: single
(D) TOPOLOGY: linear

(ii) MOLECULE TYPE:
(A) DESCRIPTION: DNA

(ix) FEATURE:
(A) NAME/KEY: G8 DNA

(xi) SEQUENCE DESCRIPTION: SEQ ID NO: 24:

GTAAGGGTGT CTGGGTCTCT TCTGGGGAAGA ACTAGAGAA TGCTGTTGGC 50

(26) INFORMATION FOR SEQ ID NO: 25:

(i) SEQUENCE CHARACTERISTICS:
(A) LENGTH: 49
(B) TYPE: nucleic acid
(C) STRANDEDNESS: single
(D) TOPOLOGY: linear

(ii) MOLECULE TYPE:
(A) DESCRIPTION: DNA

(ix) FEATURE:
(A) NAME/KEY: G8 DNA

(xi) SEQUENCE DESCRIPTION: SEQ ID NO: 25:

CTGAGTGATA TAGGTGTCTG GGTCTCTTATG ACGAATGTA ATTAAGAAC 49

(27) INFORMATION FOR SEQ ID NO: 26:

(i) SEQUENCE CHARACTERISTICS:
(A) LENGTH: 46
(B) TYPE: nucleic acid
(C) STRANDEDNESS: single
(D) TOPOLOGY: linear

(ii) MOLECULE TYPE:
(A) DESCRIPTION: DNA

(ix) FEATURE:
(A) NAME/KEY: G8 DNA

(xi) SEQUENCE DESCRIPTION: SEQ ID NO: 26:

TGTTTAGAAG CAGGCTCTTA CTTATCTTCTG GGCCTCTTT TAAGAA 46

(28) INFORMATION FOR SEQ ID NO: 27:

(i) SEQUENCE CHARACTERISTICS:
(A) LENGTH: 47
(B) TYPE: nucleic acid
(C) STRANDEDNESS: single
(D) TOPOLOGY: linear

(ii) MOLECULE TYPE:
(A) DESCRIPTION: DNA

(ix) FEATURE:
(A) NAME/KEY: G8 DNA

(xi) SEQUENCE DESCRIPTION: SEQ ID NO: 27:

TGTTTAGAGG CAGGCTCTTA ATGCTTCTGGG CCTCTTTTT TAAGAAC 47

(29) INFORMATION FOR SEQ ID NO: 28:

(i) SEQUENCE CHARACTERISTICS:
(A) LENGTH: 49
(B) TYPE: nucleic acid
(C) STRANDEDNESS: single
(D) TOPOLOGY: linear

(ii) MOLECULE TYPE:
(A) DESCRIPTION: DNA

(ix) FEATURE:
(A) NAME/KEY: G8 DNA

(xi) SEQUENCE DESCRIPTION: SEQ ID NO: 28:

GTGAGAAGTT TCAATTGGAC GTGAGTCTGGG TCTCTTTGC GTGAAGAAC 49

(30) INFORMATION FOR SEQ ID NO: 29:

(i) SEQUENCE CHARACTERISTICS:
(A) LENGTH: 39
(B) TYPE: nucleic acid
(C) STRANDEDNESS: single
(D) TOPOLOGY: linear

(ii) MOLECULE TYPE:
(A) DESCRIPTION: DNA

(ix) FEATURE:
(A) NAME/KEY: G8 DNA

(xi) SEQUENCE DESCRIPTION: SEQ ID NO: 29:

TGTTTAGAAC GAGGCTCCTA CTTCTGGCCTC TTTTAGAC 39

(31) INFORMATION FOR SEQ ID NO: 30:

(i) SEQUENCE CHARACTERISTICS:
(A) LENGTH: 50
(B) TYPE: nucleic acid
(C) STRANDEDNESS: single
(D) TOPOLOGY: linear

(ii) MOLECULE TYPE:
(A) DESCRIPTION: DNA

(ix) FEATURE:
(A) NAME/KEY: C1 DNA

(xi) SEQUENCE DESCRIPTION: SEQ ID NO: 30:

ATAGTTAAGA GCGCGTGGTA GGCGGGAACA AATGTTTACG TTGTGTAGAA 50

(32) INFORMATION FOR SEQ ID NO: 31:

(i) SEQUENCE CHARACTERISTICS:
(A) LENGTH: 50
(B) TYPE: nucleic acid
(C) STRANDEDNESS: single
(D) TOPOLOGY: linear

(ii) MOLECULE TYPE:
(A) DESCRIPTION: DNA

(ix) FEATURE:
(A) NAME/KEY: C3 DNA

(xi) SEQUENCE DESCRIPTION: SEQ ID NO: 31:

TGTTTAGAAG CAGGCTCTTA CTTATGCTTC TGGGCCTCTT TTTTAAGAAC 50

(33) INFORMATION FOR SEQ ID NO: 32:

(i) SEQUENCE CHARACTERISTICS:
(A) LENGTH: 87
(B) TYPE: nucleic acid
(C) STRANDEDNESS: single
(D) TOPOLOGY: linear

(ii) MOLECULE TYPE:
(A) DESCRIPTION: DNA

(ix) FEATURE:
(A) NAME/KEY: C1 variant DNA

(xi) SEQUENCE DESCRIPTION: SEQ ID NO: 32:

GAATTCTAAT ACGACTCACT ATAGGAAGAG ATGGCGACAT AGTTAAGAGC 50

TCGGGGTAGG CGGGAACAAC GTTCACGTTG TGTAGAA 87

(34) INFORMATION FOR SEQ ID NO: 33:

(i) SEQUENCE CHARACTERISTICS:
(A) LENGTH: 69
(B) TYPE: nucleic acid
(C) STRANDEDNESS: single
(D) TOPOLOGY: linear

(ii) MOLECULE TYPE:
(A) DESCRIPTION: DNA

(ix) FEATURE:
(A) NAME/KEY: self-cleaving DNA

(xi) SEQUENCE DESCRIPTION: SEQ ID NO: 33:

GAATTCTAAT ACGACTCACT ATAGGAAGAG ATGGCGACCT AGATTGAGTC 50

TGGGCCTCTT TTTAAGAAC 69

(35) INFORMATION FOR SEQ ID NO: 34:

(i) SEQUENCE CHARACTERISTICS:
(A) LENGTH: 46
(B) TYPE: nucleic acid
(C) STRANDEDNESS: single
(D) TOPOLOGY: linear

(ii) MOLECULE TYPE:
(A) DESCRIPTION: DNA

(ix) FEATURE:
(A) NAME/KEY: truncated class II DNA

(xi) SEQUENCE DESCRIPTION: SEQ ID NO: 34:

GAATTCTAATA CGACTCAGA ATGAGTCTGG GCCTCTTTTT AAGAAC 46

(36) INFORMATION FOR SEQ ID NO: 35:

(i) SEQUENCE CHARACTERISTICS:
(A) LENGTH: 21
(B) TYPE: nucleic acid
(C) STRANDEDNESS: single
(D) TOPOLOGY: linear

(ii) MOLECULE TYPE:
(A) DESCRIPTION: DNA

(ix) FEATURE:
(A) NAME/KEY: S3 DNA

(xi) SEQUENCE DESCRIPTION: SEQ ID NO: 35:

GAATTCTAAT ACGGCTTACC G 21

(37) INFORMATION FOR SEQ ID NO: 36:

(i) SEQUENCE CHARACTERISTICS:
(A) LENGTH: 28
(B) TYPE: nucleic acid
(C) STRANDEDNESS: single
(D) TOPOLOGY: linear

(ii) MOLECULE TYPE:
(A) DESCRIPTION: DNA

(ix) FEATURE:
(A) NAME/KEY: C3 DNA

(xi) SEQUENCE DESCRIPTION: SEQ ID NO: 36:

CGGTAAGCCT GGGCCTCTTT TTAAGAAC 28

(38) INFORMATION FOR SEQ ID NO: 37:

(i) SEQUENCE CHARACTERISTICS:
(A) LENGTH: 65
(B) TYPE: nucleic acid
(C) STRANDEDNESS: single
(D) TOPOLOGY: linear

(ii) MOLECULE TYPE:
(A) DESCRIPTION: DNA

(ix) FEATURE:
(A) NAME/KEY: DNA with 3 cleavage sites

(xi) SEQUENCE DESCRIPTION: SEQ ID NO: 37:

GTCGACCTGC GAGCTCGACT CATACGTCGA TCCCTCATGT GGCTTACCGA 50

AGCTTTACGA TCTAC 65

(39) INFORMATION FOR SEQ ID NO: 38:

(i) SEQUENCE CHARACTERISTICS:
(A) LENGTH: 58
(B) TYPE: nucleic acid
(C) STRANDEDNESS: single
(D) TOPOLOGY: linear

(ii) MOLECULE TYPE:
(A) DESCRIPTION: DNA

(ix) FEATURE:
(A) NAME/KEY: DNA with 3 cleavage sites

(xi) SEQUENCE DESCRIPTION: SEQ ID NO: 38:

GTCGACCTGCG AGCTTTCTC TTGCTCTTCT TTGCTTCTTT CTAAGCTTTA 50

CGATCTAC 58

(40) INFORMATION FOR SEQ ID NO: 39:

(i) SEQUENCE CHARACTERISTICS:
(A) LENGTH: 44
(B) TYPE: nucleic acid
(C) STRANDEDNESS: single
(D) TOPOLOGY: linear

(ii) MOLECULE TYPE:
(A) DESCRIPTION: DNA

(ix) FEATURE:
(A) NAME/KEY: portion 1
(D) OTHER INFORMATION: N is an RNA A linkage

(xi) SEQUENCE DESCRIPTION: SEQ ID NO: 39:

GAATTCTAAT ACGACTCACT NGGAAGAGAT GGCGACACAC TCTC 44

(41) INFORMATION FOR SEQ ID NO: 40:

(i) SEQUENCE CHARACTERISTICS:
(A) LENGTH: 19
(B) TYPE: nucleic acid
(C) STRANDEDNESS: single
(D) TOPOLOGY: linear

(ii) MOLECULE TYPE:
(A) DESCRIPTION: DNA

(ix) FEATURE:
(A) NAME/KEY: portion 2

(xi) SEQUENCE DESCRIPTION: SEQ ID NO: 40:

GTGAGGTTGG TGTGGTTG 19

(42) INFORMATION FOR SEQ ID NO: 41:

(i) SEQUENCE CHARACTERISTICS:

(A) LENGTH: 40
(B) TYPE: nucleic acid
(C) STRANDEDNESS: single
(D) TOPOLOGY: linear

(ii) MOLECULE TYPE:
(A) DESCRIPTION: DNA

(ix) FEATURE:
(A) NAME/KEY: class I DNA

(xi) SEQUENCE DESCRIPTION: SEQ ID NO: 41:

GTTGGGTCAC GGTATGGGGT CACTCGACGA AAATGCCGG 40

(43) INFORMATION FOR SEQ ID NO: 42:

(i) SEQUENCE CHARACTERISTICS:
(A) LENGTH: 39
(B) TYPE: nucleic acid
(C) STRANDEDNESS: single
(D) TOPOLOGY: linear

(ii) MOLECULE TYPE:
(A) DESCRIPTION: DNA

(ix) FEATURE:
(A) NAME/KEY: class II DNA

(xi) SEQUENCE DESCRIPTION: SEQ ID NO: 42:

AGGATTGGTT CTGGGTGGGGT AGGAGTTAG TGTGATCCG 39

(44) INFORMATION FOR SEQ ID NO: 43:

(i) SEQUENCE CHARACTERISTICS:
(A) LENGTH: 40
(B) TYPE: nucleic acid
(C) STRANDEDNESS: single
(D) TOPOLOGY: linear

(ii) MOLECULE TYPE:
(A) DESCRIPTION: DNA

(ix) FEATURE:
(A) NAME/KEY: class III DNA

(xi) SEQUENCE DESCRIPTION: SEQ ID NO: 43:

CGGGTCGAGG TGGGGAAAAC AGGCAAGGCT GTTCAGGATG 40

(45) INFORMATION FOR SEQ ID NO: 44:

(i) SEQUENCE CHARACTERISTICS:
(A) LENGTH: 40
(B) TYPE: nucleic acid
(C) STRANDEDNESS: single
(D) TOPOLOGY: linear

(ii) MOLECULE TYPE:
(A) DESCRIPTION: DNA

(ix) FEATURE:
(A) NAME/KEY: class IV DNA

(xi) SEQUENCE DESCRIPTION: SEQ ID NO: 44:

AGGATTAAGC CGAATTCCAG CACACTGGCG GCCGCTTCAC 40

(46) INFORMATION FOR SEQ ID NO: 45:

(i) SEQUENCE CHARACTERISTICS:
(A) LENGTH: 38
(B) TYPE: nucleic acid
(C) STRANDEDNESS: single
(D) TOPOLOGY: linear

(ii) MOLECULE TYPE:
(A) DESCRIPTION: DNA

(ix) FEATURE:
(A) NAME/KEY: class II DNA

(xi) SEQUENCE DESCRIPTION: SEQ ID NO: 45:

AGGATTGGTT CTGGGTGGGT AGGAAGTTAG TGTGAGCC 38

(47) INFORMATION FOR SEQ ID NO: 46:

(i) SEQUENCE CHARACTERISTICS:
(A) LENGTH: 31
(B) TYPE: nucleic acid
(C) STRANDEDNESS: single
(D) TOPOLOGY: linear

(ii) MOLECULE TYPE:
(A) DESCRIPTION: DNA

(ix) FEATURE:
(A) NAME/KEY: HD2 pool DNA

(xi) SEQUENCE DESCRIPTION: SEQ ID NO: 46:

TTGATCGGGG CTGTGCGGGT AGGAAGTAAT A 31

(48) INFORMATION FOR SEQ ID NO: 47:

(i) SEQUENCE CHARACTERISTICS:
(A) LENGTH: 67
(B) TYPE: nucleic acid
(C) STRANDEDNESS: single
(D) TOPOLOGY: linear

(ii) MOLECULE TYPE:
(A) DESCRIPTION: DNA

(ix) FEATURE:
(A) NAME/KEY: HD1
(D) OTHER INFORMATION: N is an RNA A linkage

(xi) SEQUENCE DESCRIPTION: SEQ ID NO: 47:

CGACTCACA TNGGAAGAGA TGCATCTCGC AGTTGGGTCT GGTTGGGTAG 50

GAAGTTAAT GTGAGACG 67

(49) INFORMATION FOR SEQ ID NO: 48:

(i) SEQUENCE CHARACTERISTICS:
(A) LENGTH: 65
(B) TYPE: nucleic acid
(C) STRANDEDNESS: single
(D) TOPOLOGY: linear

(ii) MOLECULE TYPE:
(A) DESCRIPTION: DNA

(ix) FEATURE:
(A) NAME/KEY: HD2
(D) OTHER INFORMATION: N is an RNA A linkage

(xi) SEQUENCE DESCRIPTION: SEQ ID NO: 48:

CGACTCACTA TNGGAAGAGA TGCATCTCTT GATCGGGGGC TGTGCGGGTA 50

GGAAGTAATA GTGAG 65

(50) INFORMATION FOR SEQ ID NO: 49:

(i) SEQUENCE CHARACTERISTICS:
(A) LENGTH: 39
(B) TYPE: nucleic acid
(C) STRANDEDNESS: single
(D) TOPOLOGY: linear

(ii) MOLECULE TYPE:
(A) DESCRIPTION: DNA

(ix) FEATURE:
(A) NAME/KEY: primer

(xi) SEQUENCE DESCRIPTION: SEQ ID NO: 49:

GAATTCTAAT ACGACTCACTA TAGGCGAAAG CCGGGCGA 39

(51) INFORMATION FOR SEQ ID NO: 50:

(i) SEQUENCE CHARACTERISTICS:
(A) LENGTH: 16
(B) TYPE: nucleic acid
(C) STRANDEDNESS: single
(D) TOPOLOGY: linear

(ii) MOLECULE TYPE:
(A) DESCRIPTION: DNA

(ix) FEATURE:
(A) NAME/KEY: primer

(xi) SEQUENCE DESCRIPTION: SEQ ID NO: 50:

GAGCTCTCG CTACCGT 16

(52) INFORMATION FOR SEQ ID NO: 51:

(i) SEQUENCE CHARACTERISTICS:
(A) LENGTH: 18
(B) TYPE: nucleic acid
(C) STRANDEDNESS: single
(D) TOPOLOGY: linear

(ii) MOLECULE TYPE:
(A) DESCRIPTION: DNA

(ix) FEATURE:
(A) NAME/KEY: primer

(xi) SEQUENCE DESCRIPTION: SEQ ID NO: 51:

GTCGACCTGC GAGCTCGA 18

(53) INFORMATION FOR SEQ ID NO: 52:

(i) SEQUENCE CHARACTERISTICS:
(A) LENGTH: 18
(B) TYPE: nucleic acid
(C) STRANDEDNESS: single
(D) TOPOLOGY: linear

(ii) MOLECULE TYPE:

(A) DESCRIPTION: DNA

(ix) FEATURE:
(A) NAME/KEY: primer

(xi) SEQUENCE DESCRIPTION: SEQ ID NO: 52:

GTAGATCGTA AAGCTTCG 18

(54) INFORMATION FOR SEQ ID NO: 53:

(i) SEQUENCE CHARACTERISTICS:
(A) LENGTH: 38
(B) TYPE: nucleic acid
(C) STRANDEDNESS: single
(D) TOPOLOGY: linear

(ii) MOLECULE TYPE:
(A) DESCRIPTION: DNA

(ix) FEATURE:
(A) NAME/KEY: template, part 1

(xi) SEQUENCE DESCRIPTION: SEQ ID NO: 53:

CTAATACGAC TCACTATAGG AAGAGATGGC GACATCTC 38

(55) INFORMATION FOR SEQ ID NO: 54:

(i) SEQUENCE CHARACTERISTICS:
(A) LENGTH: 18
(B) TYPE: nucleic acid
(C) STRANDEDNESS: single
(D) TOPOLOGY: linear

(ii) MOLECULE TYPE:
(A) DESCRIPTION: DNA

(ix) FEATURE:
(A) NAME/KEY: template, part 2

(xi) SEQUENCE DESCRIPTION: SEQ ID NO: 54:

GTGAGGTTGG TGTGGTTG 18

(56) INFORMATION FOR SEQ ID NO: 55:

(i) SEQUENCE CHARACTERISTICS:
(A) LENGTH: 23
(B) TYPE: nucleic acid
(C) STRANDEDNESS: single
(D) TOPOLOGY: linear

(ii) MOLECULE TYPE:
(A) DESCRIPTION: DNA

(ix) FEATURE:
(A) NAME/KEY: primer
(D) OTHER INFORMATION: N is an RNA A

(xi) SEQUENCE DESCRIPTION: SEQ ID NO: 55:

GAATTCTAAT ACGACTCACT ATN 23

(57) INFORMATION FOR SEQ ID NO: 56:

(i) SEQUENCE CHARACTERISTICS:
(A) LENGTH: 18
(B) TYPE: nucleic acid
(C) STRANDEDNESS: single
(D) TOPOLOGY: linear

(ii) MOLECULE TYPE:
(A) DESCRIPTION: DNA

(ix) FEATURE:
(A) NAME/KEY: primer

(xi) SEQUENCE DESCRIPTION: SEQ ID NO: 56:

CAACCACACC AACCTCAC 18

(58) INFORMATION FOR SEQ ID NO: 57:

(i) SEQUENCE CHARACTERISTICS:
(A) LENGTH: 38
(B) TYPE: nucleic acid
(C) STRANDEDNESS: single
(D) TOPOLOGY: linear

(ii) MOLECULE TYPE:
(A) DESCRIPTION: DNA

(ix) FEATURE:
(A) NAME/KEY: primer

(xi) SEQUENCE DESCRIPTION: SEQ ID NO: 57:

GAATTCTAAT ACGACTCACT ATAGGAAGAG ATGGCGAC 38

CLAIMS

1. A purified functional DNA polynucleotide that exhibits allosteric properties that modify a function or configuration of the polynucleotide with a chemical effector, a physical signal, or combinations thereof.

2. A polynucleotide according to claim 1 which is an enzyme exhibiting allosteric properties that modify the rate of catalysis of the enzyme.

3. A purified functional polynucleotide having catalytic properties with rates that can be controlled by a chemical effector, a physical signal, or combinations thereof.

4. A polynucleotide according to claim 3 comprising DNA.

5. A polynucleotide according to claim 3 comprising RNA.

6. A polynucleotide according to claims 1, 2, 3, 4, or 5 comprising a sequence selected from the group consisting of SEQ ID NOs 1, 3 to 6, and 9 to 48.

7. A polynucleotide according to claims 1, 2, 3, 4, or 5 wherein the chemical effectors are selected from the group consisting of organic compounds and mixtures of organic compounds and metal ions.

8. A polynucleotide according to claim 7 wherein the chemical effectors are selected from the group consisting of amino acids, amino acid derivatives, peptides, nucleosides, nucleotides, steroids, and mixtures thereof.

9. A polynucleotide according to claims 1, 2, 3, 4, or 5 wherein the chemical effectors are microbial or cellular metabolites or blood or urine components or other bodily fluids obtained from biological samples.

10. A polynucleotide according to claims 1, 2, 3, 4, or 5 wherein the chemical effectors are pharmaceuticals.

11. A polynucleotide according to claims 1, 2, 3, 4, or 5 wherein the chemical effectors are selected from the group consisting of pesticides, herbicides, food toxins, and mixtures thereof.

12. A polynucleotide according to claims 1, 2, 3, 4, or 5 wherein the physical signals are selected from the group consisting of radiation, a temperature change, and combinations thereof.

13. A biosensor comprising a polynucleotide according to claims 1, 2, 3, 4, 5, or 8.

14. A biosensor according to claim 13 attached to a solid support.

15. A solid support to which is attached a polynucleotide according to claims 1, 2, 3, 4, 5, or 8.

16. A method for detecting the presence or absence of a compound or its concentration in a sample comprising contacting the sample with a polynucleotide according to claims 1, 2, 3, 4, 5, or 8.

17. A method according to claim 16 wherein the presence or absence of a compound or its concentration is detected by observation of polynucleotide self-cleavage.

18. A method according to claim 16 wherein the presence or concentration of a compound is detected by observation of a change in polynucleotide configuration or function.

19. A method for detecting the presence or absence of a physical change in a sample comprising contacting the sample with a polynucleotide according to claims 1, 2, 3, 4 5, or 8.

20. A method according to claim 19 wherein the presence of a physical change is detected by observation of polynucleotide self-cleavage.

21. A method according to claim 19 wherein the presence of a physical change in a sample is detected by observation of a change in polynucleotide configuration or function.

22. A biosensor comprising a polynucleotide exhibiting allosteric properties that modify a function or configuration of the polynucleotide with a chemical effector, a physical signal, or combinations thereof.

23. A biosensor comprising a catalytic polynucleotide.

24. A biosensor according to claims 22 or 23 wherein the polynucleotide comprises DNA.

25. A biosensor according to claims 22 or 23 wherein the polynucleotide comprises RNA.

26. A biosensor according to claims 22 or 23 wherein the polynucleotide has self-cleaving activity.

27. A biosensor according to claims 22 or 23 wherein the catalytic or allosteric properties of the polynucleotide are controlled by a chemical effector.

28. A biosensor according to claim 27 wherein the chemical effectors are selected from the group consisting of organic compounds and mixtures of organic compounds and metal ions.

29. A biosensor according to claim 27 wherein the chemical effectors are selected from the group consisting of amino acids, amino acid derivatives, peptides, nucleosides, nucleotides, steroids, and mixtures thereof.

30. A biosensor according to claim 27 wherein the chemical effectors are microbial or cellular metabolites or blood or urine components or other bodily fluids obtained from biological samples.

31. A biosensor according to claim 27 wherein the chemical effectors are pharmaceuticals.

32. A biosensor according to claim 27 wherein the chemical effectors are selected from the group consisting of pesticides, herbicides, food toxins, and mixtures thereof.

33. A biosensor according to claims 22 or 23 wherein the catalytic or allosteric properties of the polynucleotide are controlled by a physical signal selected from the group consisting of radiation, a temperature change and combinations thereof.

34. A biosensor according to claims 22, 23, 28, 29, 30, 31, or 32 wherein the polynucleotide is attached to a solid support.

35. A method for detecting the presence or absence of a compound or its concentration in a sample comprising contacting the sample with a biosensor according to claims 22, 23, 28, 29, 30, 31, or 32 and observing a change in the functional properties or configuration of the polynucleotide.

36. A method for detecting the presence or absence of a physical change in a sample comprising contacting the sample with a biosensor according to claims 22, 23. 28, 29, 30, 31, or 32 and observing a change in the functional properties or configuration of the polynucleotide.

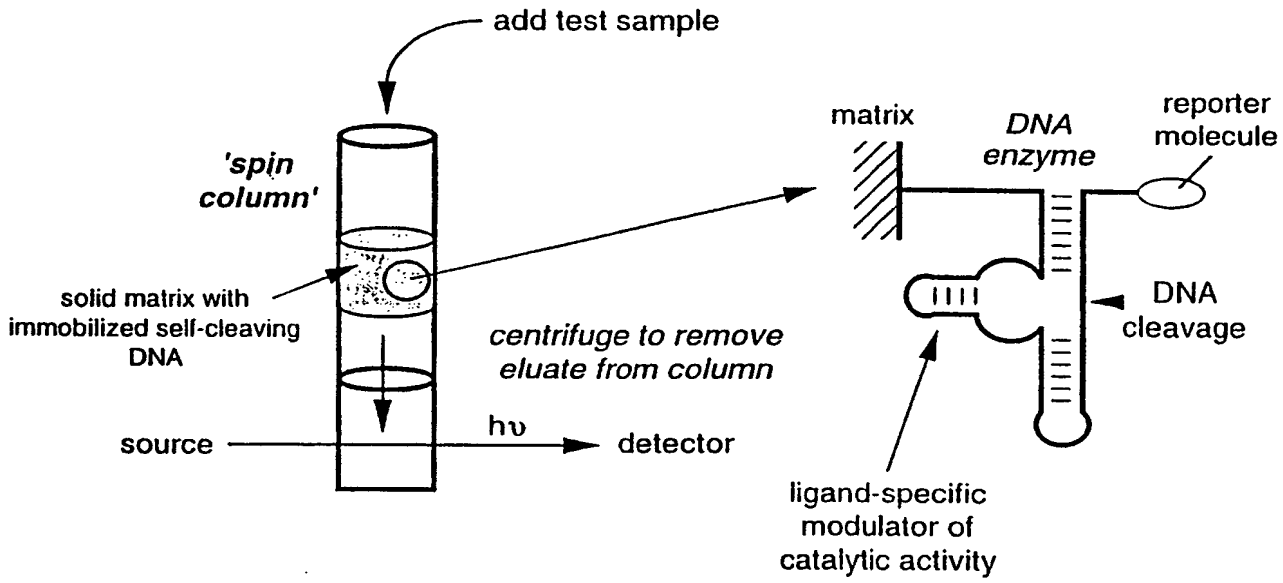

Figure 1

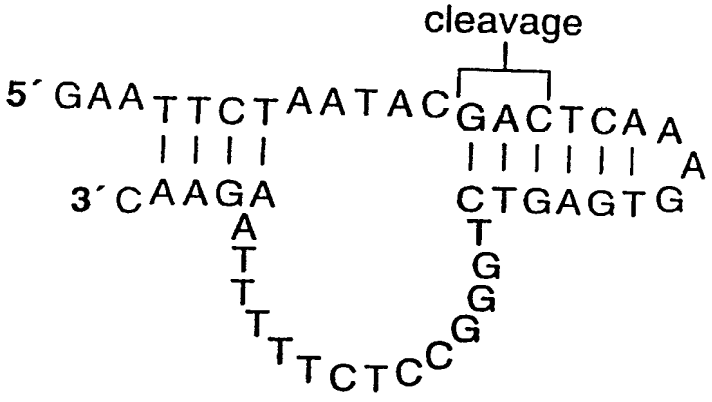

Figure 2

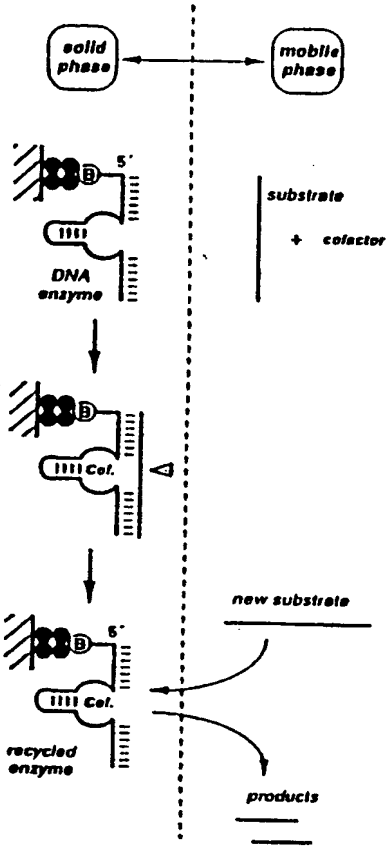

Figure 3A

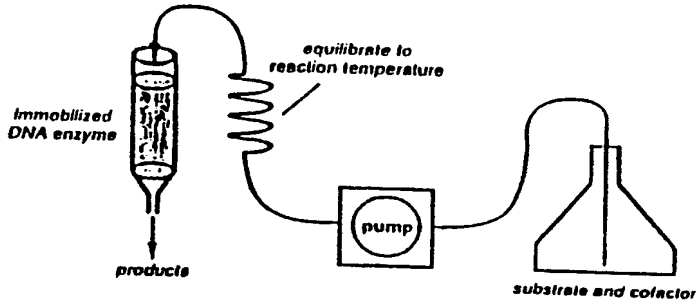

Figure 3B

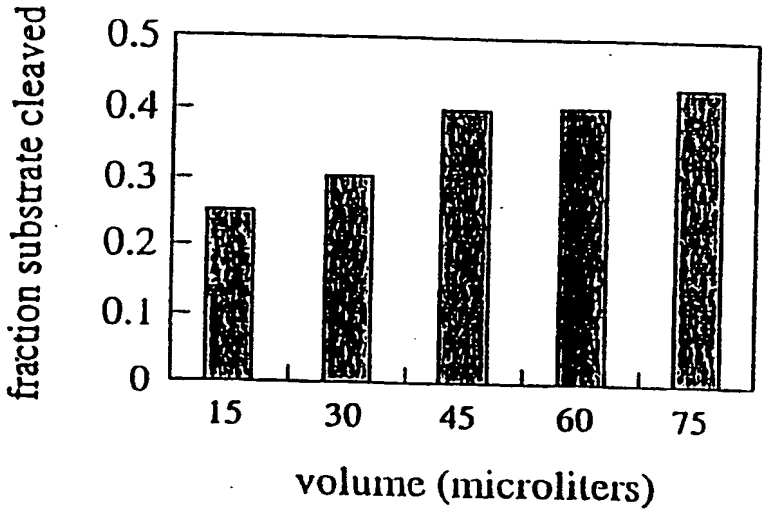

Figure 4

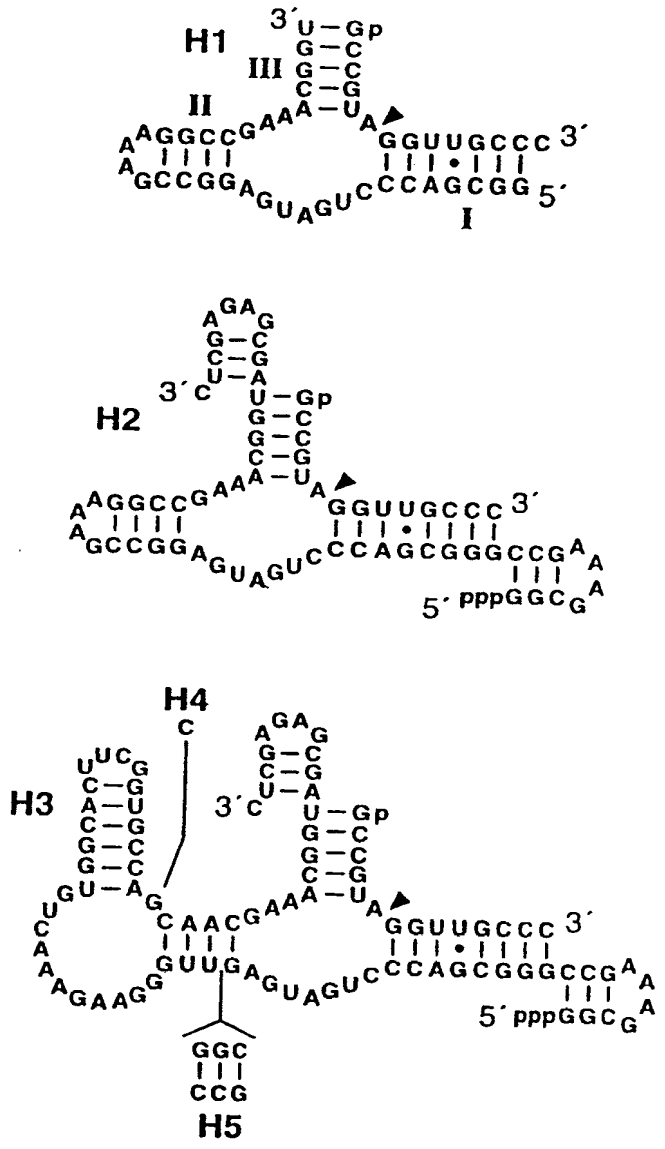

Figure 5

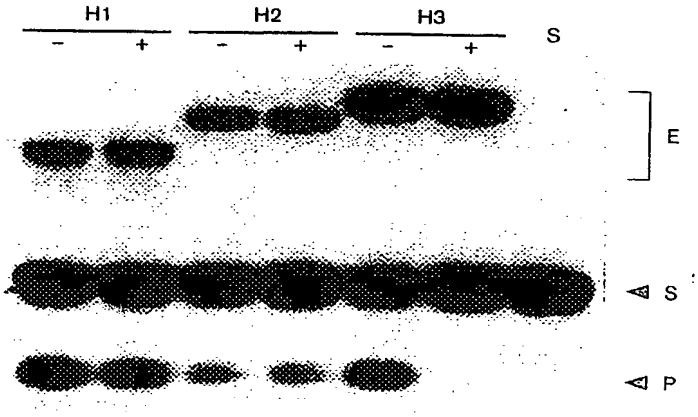

Figure 6A

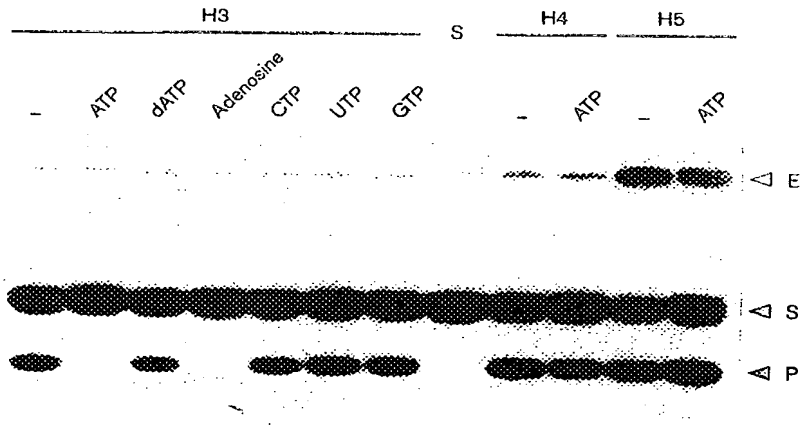

Figure 6B

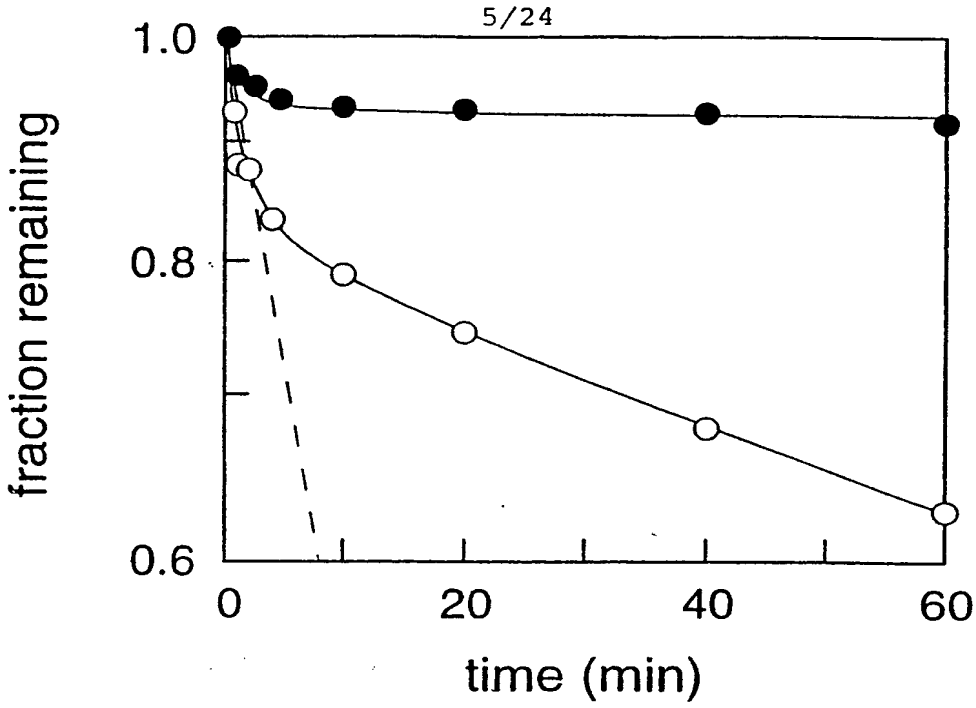

Figure 7A

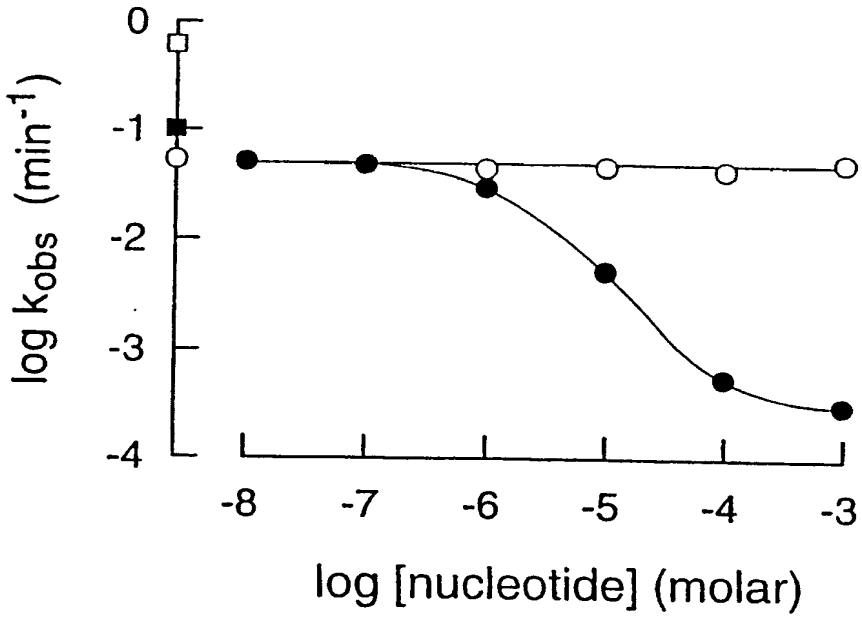

Figure 7B

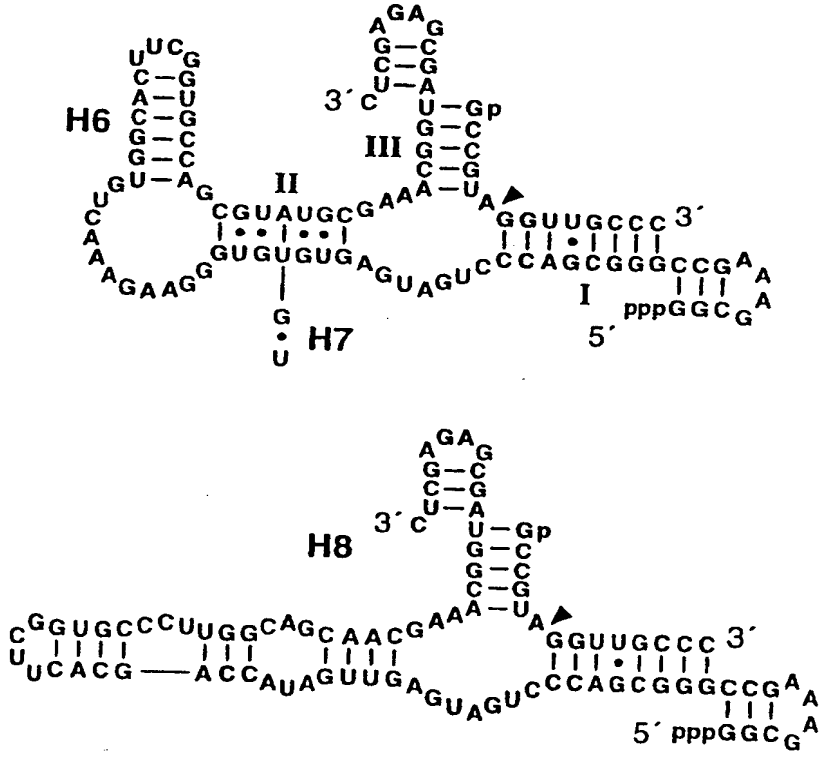

Figure 8A

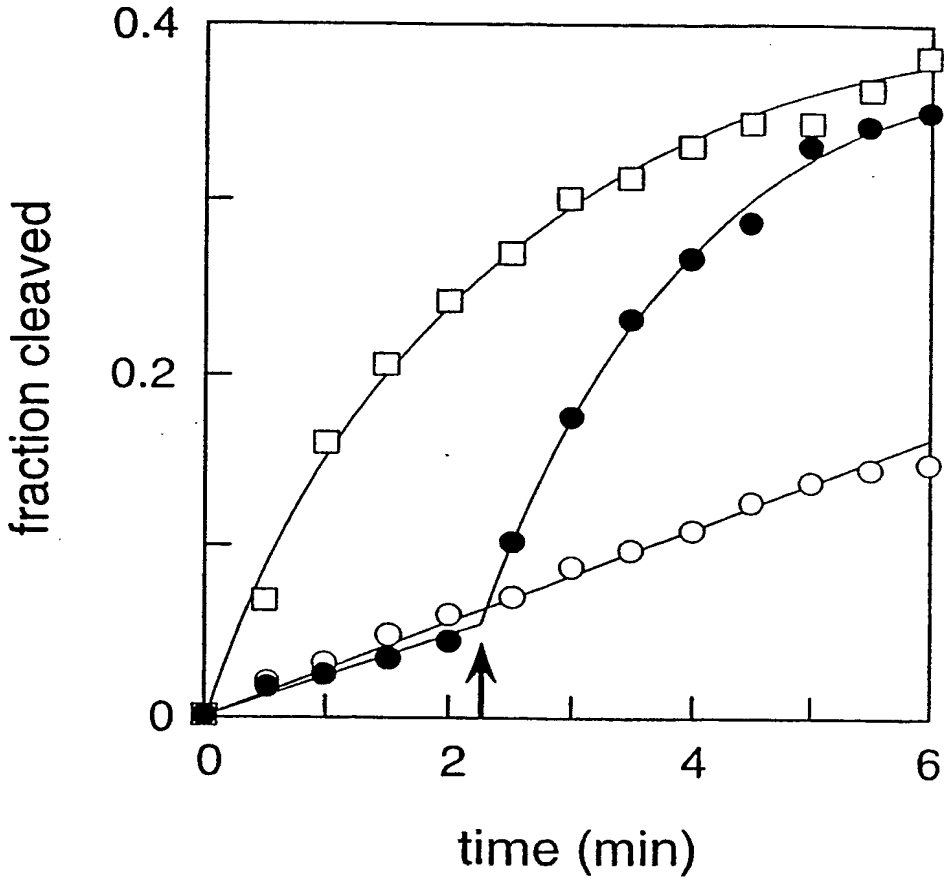

Figure 8B

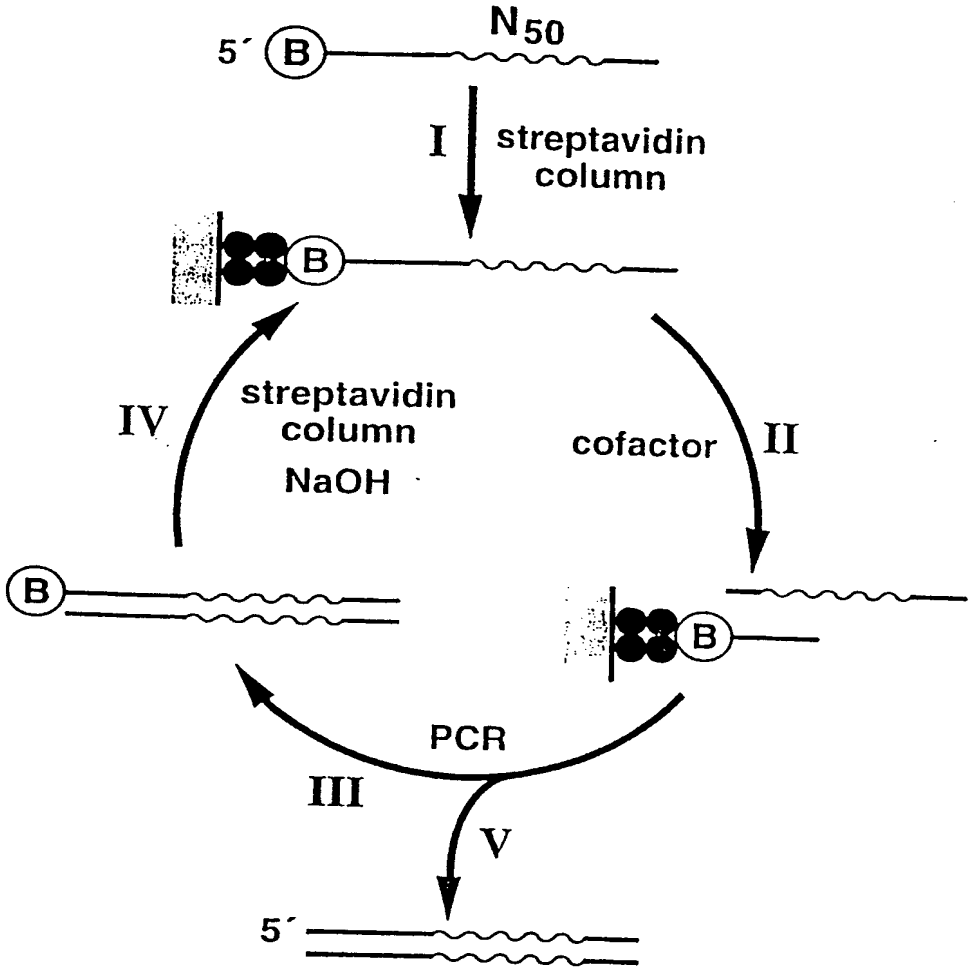
5´
B
N50
I
streptavidin
column
B
IV
streptavidin
column
NaOH
cofactor
II
B
B
PCR
III
V
5´

Figure 9A

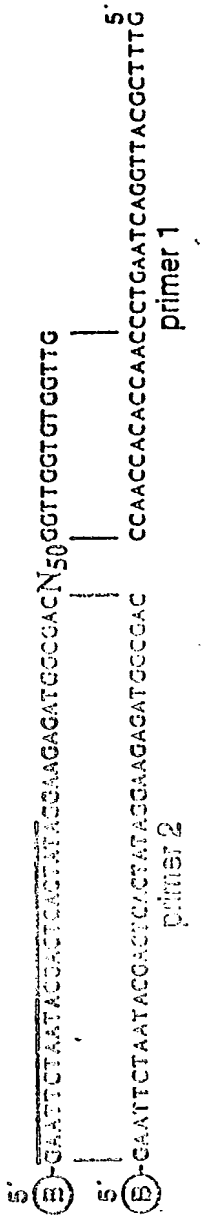

Figure 9B

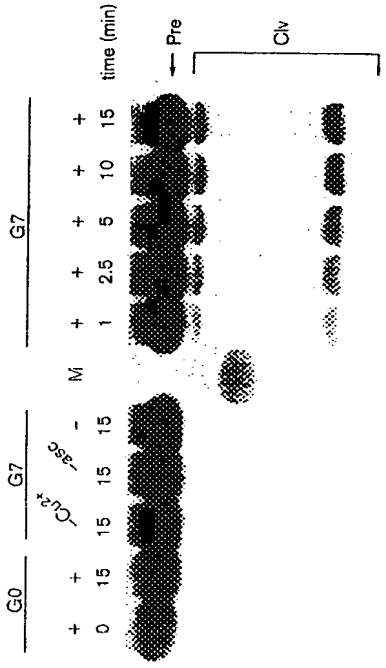

Figure 9C

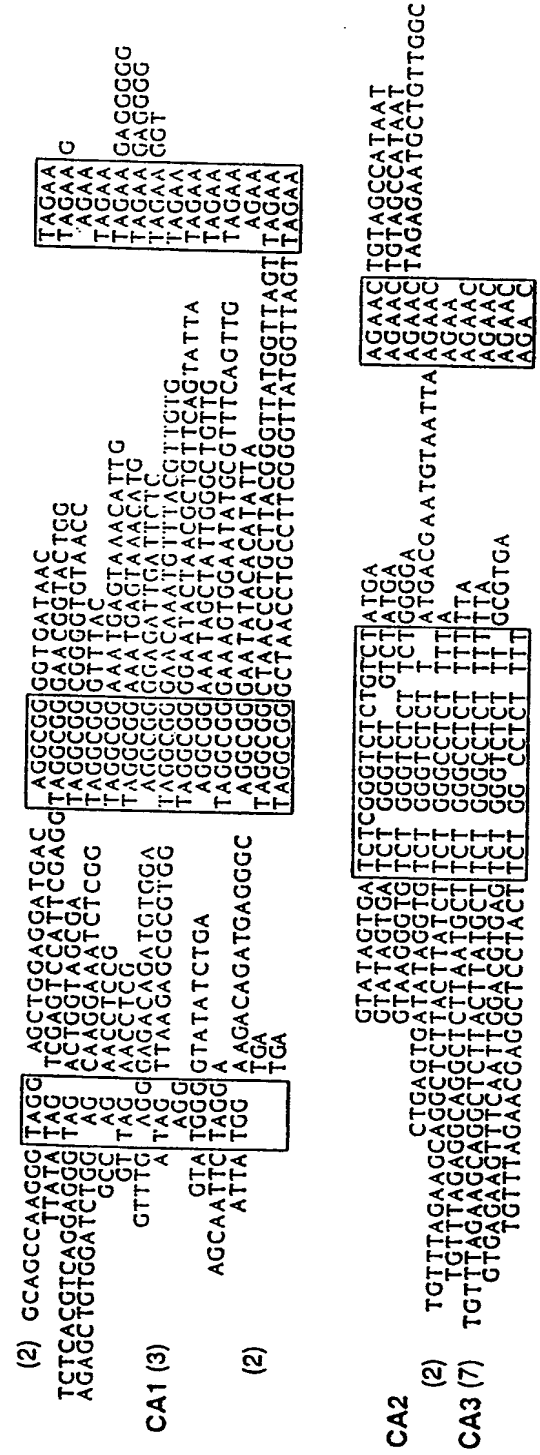

Figure 10A

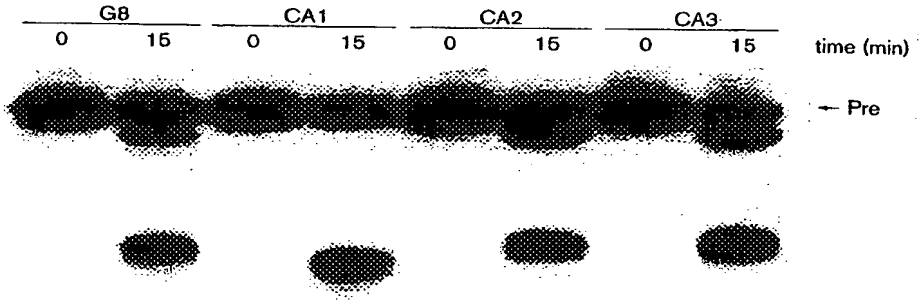

Figure 10B

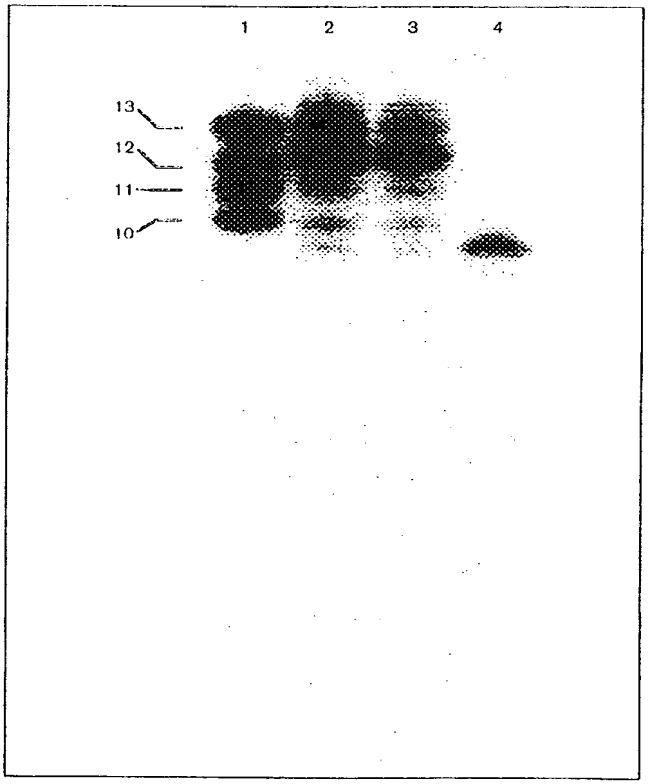

Figure 11

Figure 12A

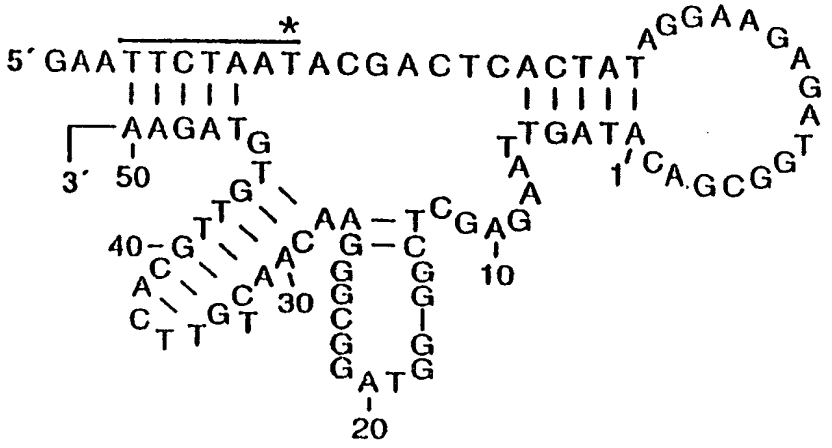

Figure 12B

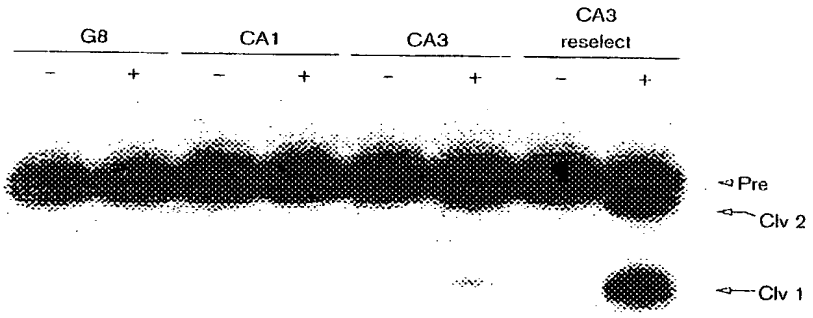

Figure 13A

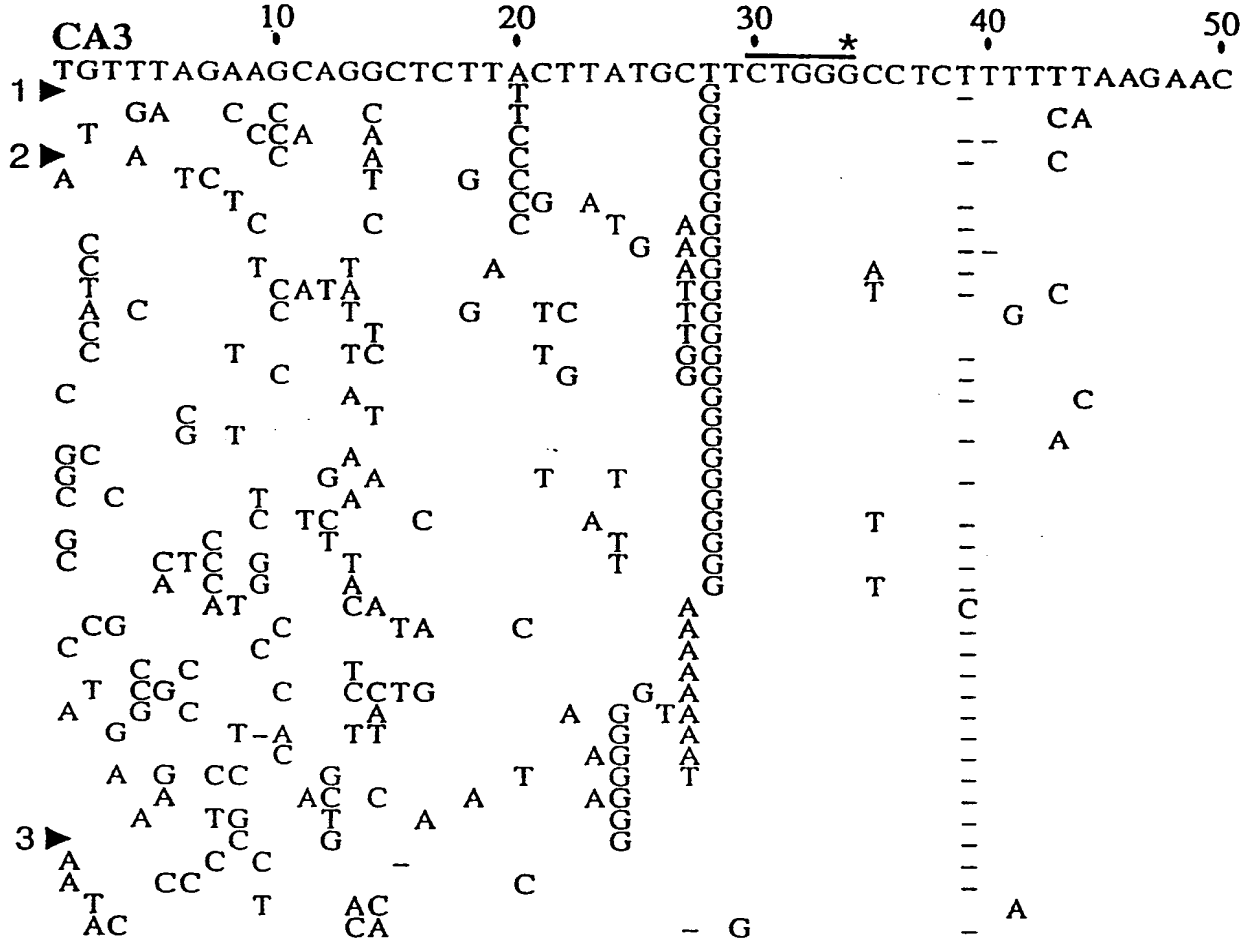

Figure 13B

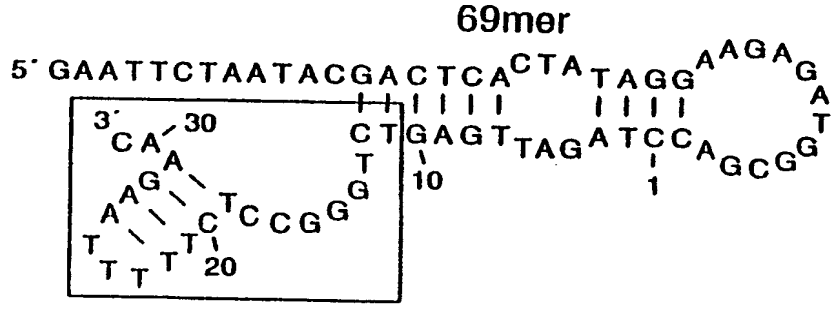

Figure 14A

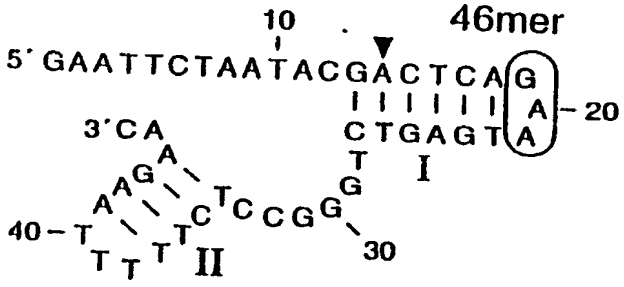

Figure 14B

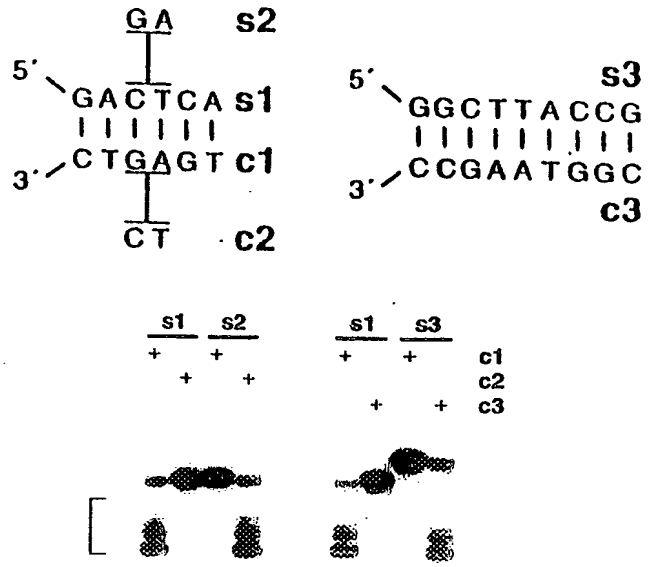

Figure 15A

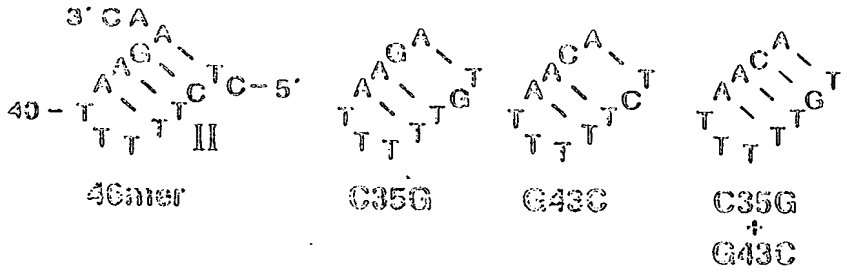

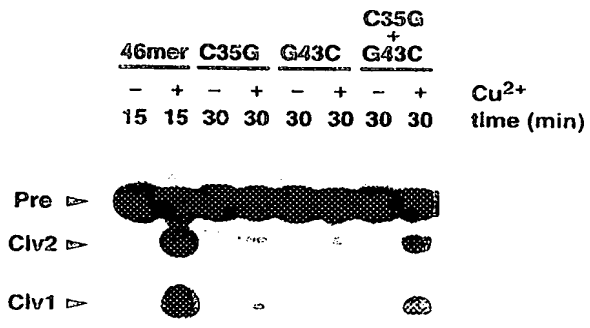

Figure 15B

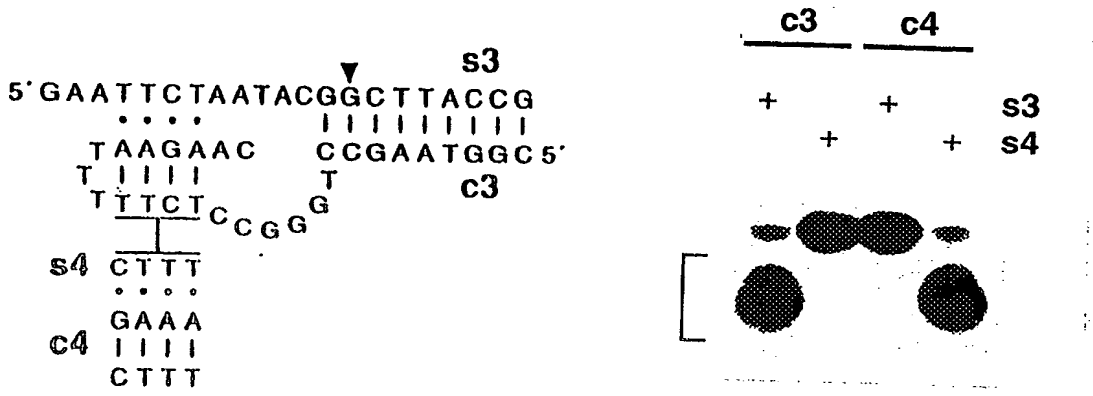

Figure16

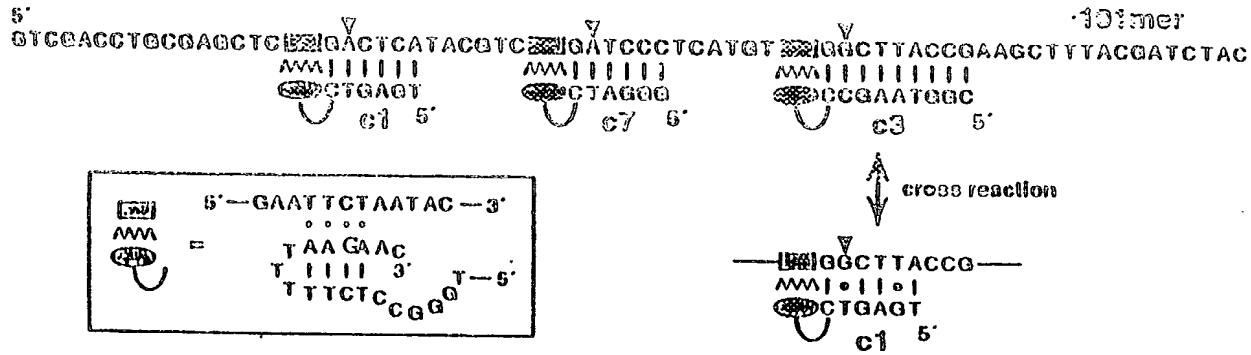

Figure 17A

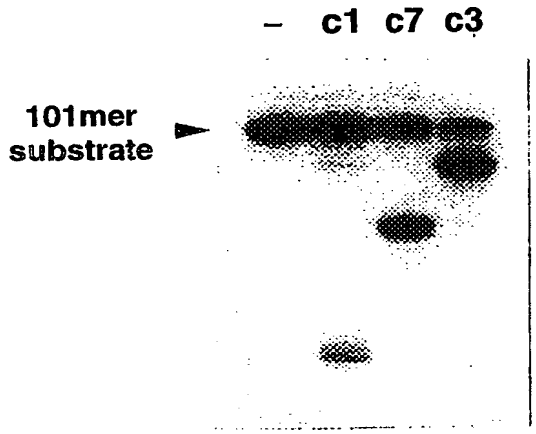

Figure 17B

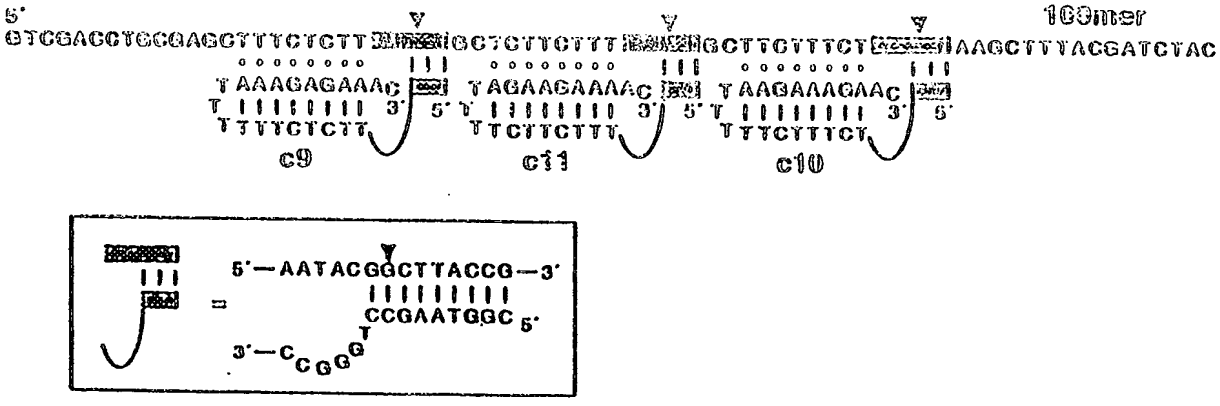

Figure 17C

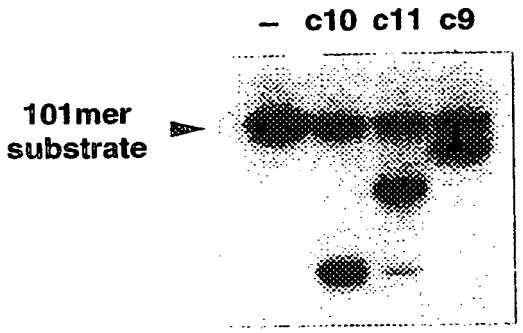

Figure 17D

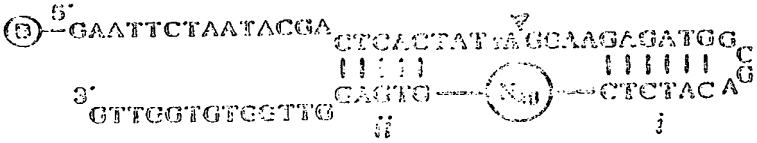

Figure 18A

class					catalytic activity HEPES	catalytic activity histidine
	10	20	30	40		
I	(7) GTTGGGTCAC	GGTATGGGGT	CACTCGACGA	AAATGCCGG	+	+
II	(6) AGGATTGGTT	CTGGGTGGGT	AGGAAGTTAG	TGTGAGCCG	–	+
III	(4) CGGGTCGAGG	TGGGGAAAAC	AGGCAAGGCT	GTTCAGGATG	+	+
IV	(3) AGGATTAAGC	CGAATTCCAG	CACACTGGCG	GCCGCTTCAC	+	+

Figure 18B

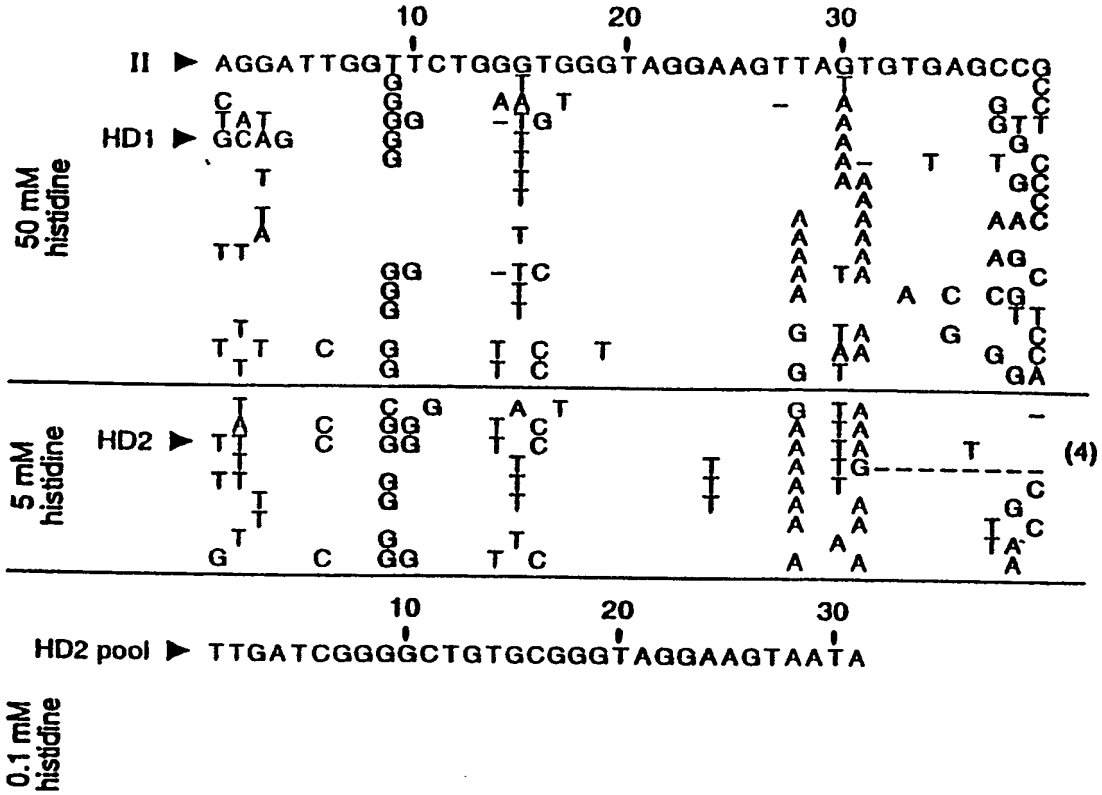

Figure 19A

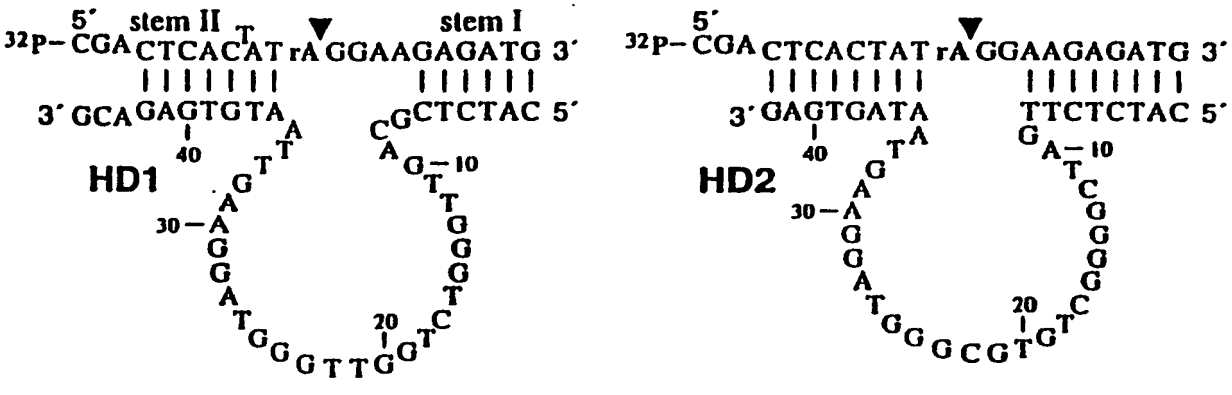

Figure 19B

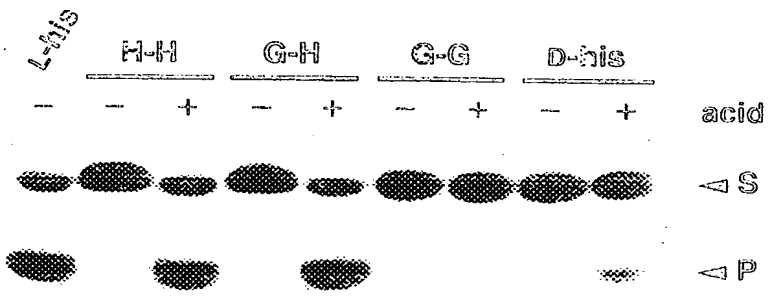

Figure 20A

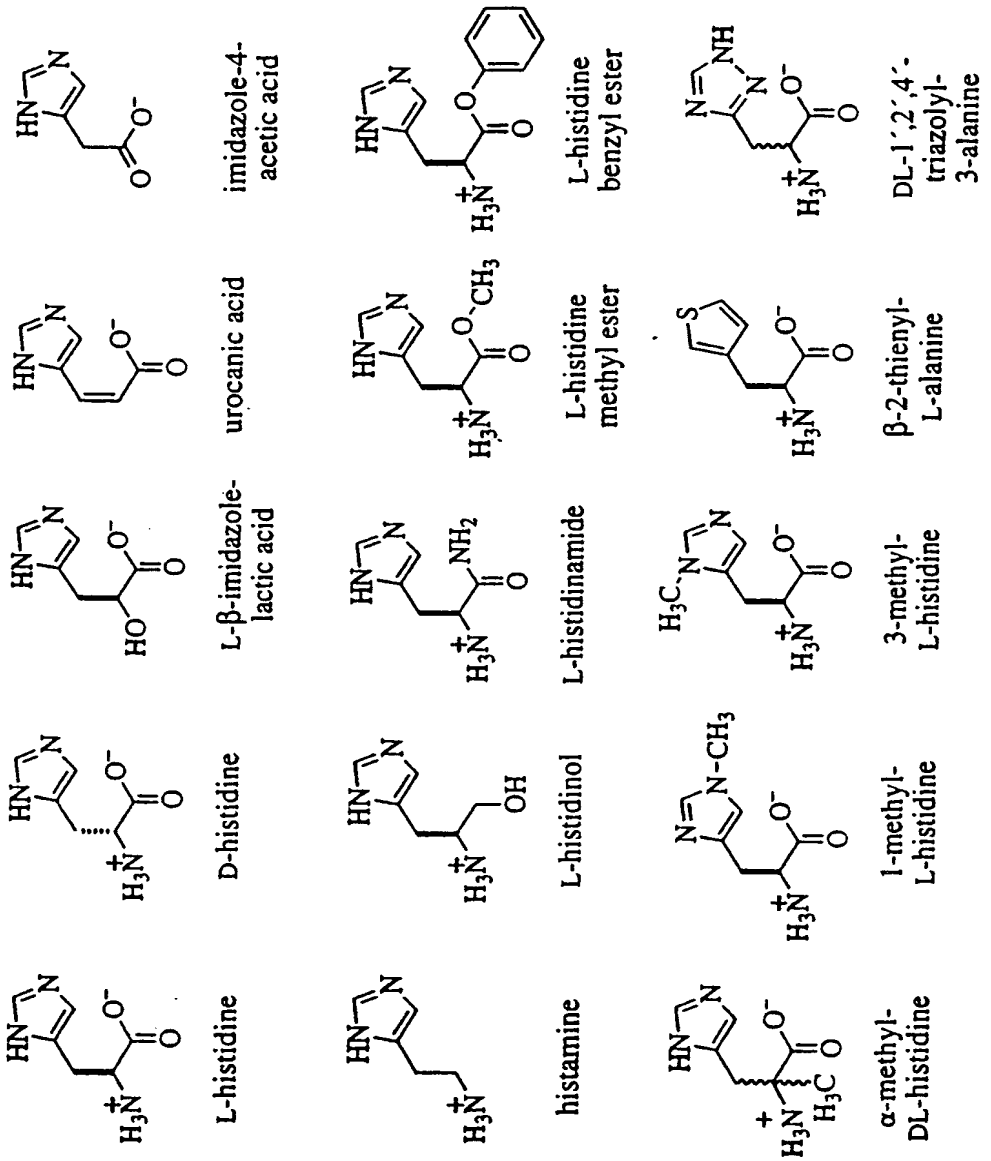

Figure 20B

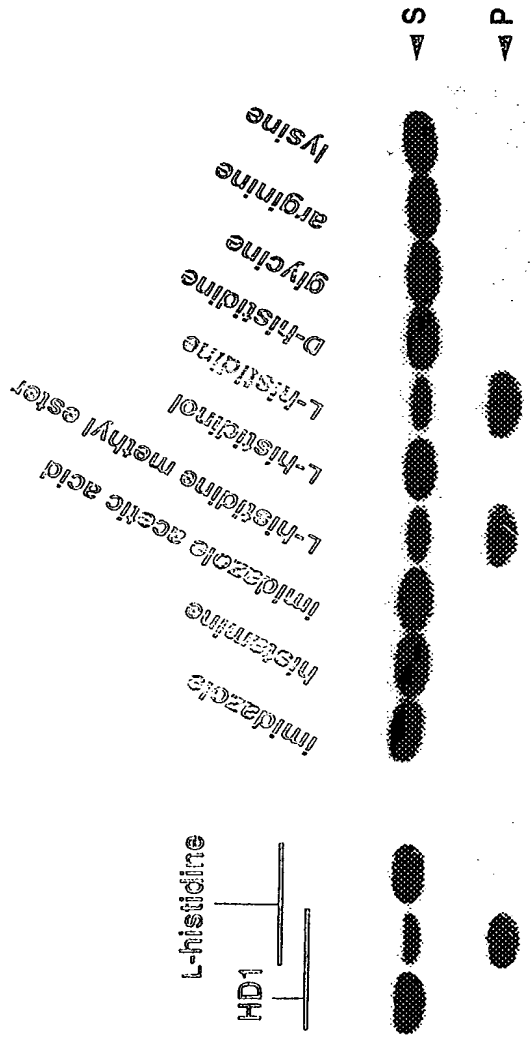

Figure 20C

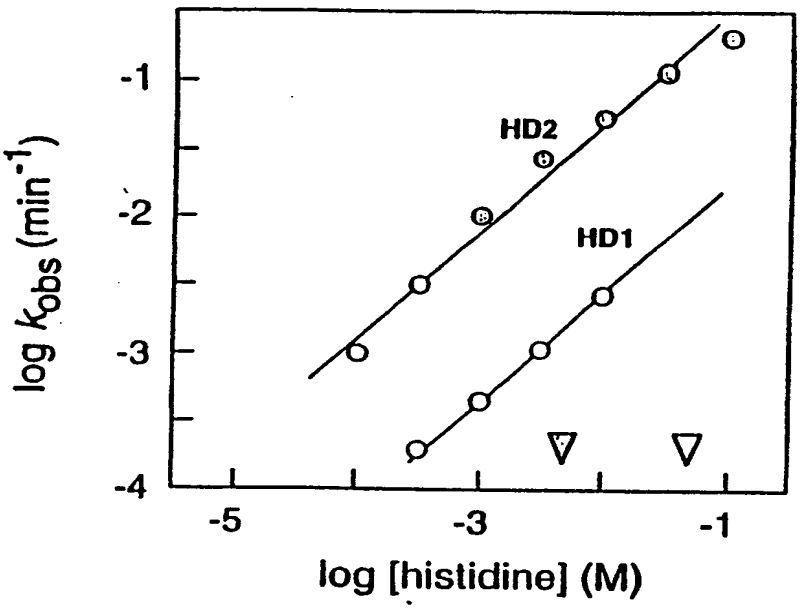

Figure 21A

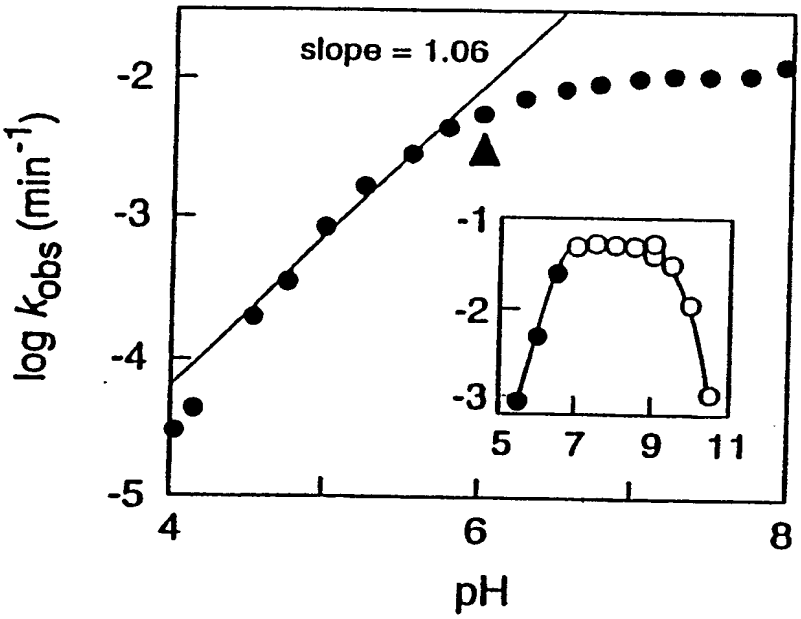

Figure 21B

INTERNATIONAL SEARCH REPORT

International application No.
PCT/US97/24158

A. CLASSIFICATION OF SUBJECT MATTER
IPC(6) :C07H 21/00
US CL :536/22.1
According to International Patent Classification (IPC) or to both national classification and IPC

B. FIELDS SEARCHED

Minimum documentation searched (classification system followed by classification symbols)

U.S. : 422/50, 68.1; 435/6; 536/22.1, 23.1, 24.1, 24.3, 25.3; 935/77, 78

Documentation searched other than minimum documentation to the extent that such documents are included in the fields searched

Electronic data base consulted during the international search (name of data base and, where practicable, search terms used)

Please See Extra Sheet.

C. DOCUMENTS CONSIDERED TO BE RELEVANT

Category*	Citation of document, with indication, where appropriate, of the relevant passages	Relevant to claim No.
Y	SCHENA, M. Parallel human genome analysis: Microarray-based expression monitoring of 1000 genes. Proceedings of the National Academy of Sciences, USA. October 1996, Volume 93, pages 10614-10619, see especially the abstract and the Discussion section in pages 10617-10619.	1-12, 15-21, 35, 36
Y	PEASE, A. C., et al. Light-generated oligonucleotide arrays for rapid DNA sequence analysis. Proceedings of the National Academy of Sciences, USA. May 1994, Volume 91, pages 5022-5026, see especially the abstract.	1-12, 15-21, 35, 36

[X] Further documents are listed in the continuation of Box C. [ ] See patent family annex.

*	Special categories of cited documents:	"T"	later document published after the international filing date or priority date and not in conflict with the application but cited to understand the principle or theory underlying the invention
"A"	document defining the general state of the art which is not considered to be of particular relevance	"X"	document of particular relevance; the claimed invention cannot be considered novel or cannot be considered to involve an inventive step when the document is taken alone
"B"	earlier document published on or after the international filing date	"Y"	document of particular relevance; the claimed invention cannot be considered to involve an inventive step when the document is combined with one or more other such documents, such combination being obvious to a person skilled in the art
"L"	document which may throw doubts on priority claim(s) or which is cited to establish the publication date of another citation or other special reason (as specified)	"&"	document member of the same patent family
"O"	document referring to an oral disclosure, use, exhibition or other means		
"P"	document published prior to the international filing date but later than the priority date claimed		

Date of the actual completion of the international search 29 MARCH 1998	Date of mailing of the international search report 05 MAY 1998
Name and mailing address of the ISA/US Commissioner of Patents and Trademarks Box PCT Washington, D.C. 20231 Facsimile No. (703) 305-3230	Authorized officer ARDIN MARSCHEL Telephone No. (703) 308-0196

Form PCT/ISA/210 (second sheet)(July 1992)*

INTERNATIONAL SEARCH REPORT

International application No.
PCT/US97/24158

C (Continuation). DOCUMENTS CONSIDERED TO BE RELEVANT

Category*	Citation of document, with indication, where appropriate, of the relevant passages	Relevant to claim No.
Y	US 5,474,911 A (PONTIUS) 12 December 1995, see especially column 6, line 44, through column 17, line 30.	1-12, 15-21, 35, 36
Y	US 5,445,934 A (FODOR et al.) 29 August 1995, see especially Figures 1-20.	1-36
Y,P	US 5,605,662 A (HELLER et al.) 25 February 1997, see especially the abstract and Figures 1-14f.	1-36
Y	US 5,143,854 A (PIRRUNG et al.) 01 September 1992, see especially the abstract and Figures 1-20.	1-36

INTERNATIONAL SEARCH REPORT

International application No.
PCT/US97/24158

B. FIELDS SEARCHED
Electronic data bases consulted (Name of data base and where practicable terms used):

APS, CAS, MEDLINE, EMBASE, WPI, BIOTECH ABS., AND BIOSIS
search terms: allosteric, biosensor, DNA, RNA, hybridize, activity, and catalytic